

**A COMPREHENSIVE MODEL FOR STUDYING THE
SUPPRESSION OF FOUR WAVE MIXING IN WDM
OPTICAL TRANSMISSION SYSTEM**

By

Shamim Al Mamun

MASTER OF SCIENCE IN INFORMATION AND COMMUNICATION TECHNOLOGY

Institute of Information and Communication Technology

Bangladesh University of Engineering and Technology

March, 2012

This thesis titled “**A Comprehensive Model for Studying the Suppression of Four Wave Mixing in WDM Optical Transmission System**” Submitted by **Shamim Al Mamun, Roll No:M10053107P, Session: October 2005** has been accepted as satisfactory in partial fulfillment of the requirements for the degree of Master of Science in Information and Communication Technology on 31 March, 2012.

BOARD OF EXAMINERS

- | | | |
|----|--|-------------------------|
| 1. | <hr/> <p>Dr.Md. Saiful Islam
Professor
Institute of Information and Communication Technology
BangladeshUniversity of Engineering and Technology
Dhaka-1000, Bangladesh</p> | Chairman |
| 2. | <hr/> <p>Dr. S. M. Lutful Kabir
Professor and Director
Institute of Information and Communication Technology
BangladeshUniversity of Engineering and Technology
Dhaka-1000, Bangladesh</p> | Member
(Ex-Officio) |
| 3. | <hr/> <p>Dr.Md. Liakot Ali
Professor
Institute of Information and Communication Technology
BangladeshUniversity of Engineering and Technology
Dhaka-1000, Bangladesh</p> | Member |
| 4. | <hr/> <p>Dr. Subrata Kumar Aditya
Professor
Dept. of Applied Physics, Electronics and Communication Engineering
University of Dhaka
Dhaka-1000, Bangladesh.</p> | Member
(External) |

DECLARATION

It is hereby declared that this thesis or any part of it has not been submitted elsewhere for the award of any degree or diploma.

Shamim Al Mamun

TABLE OF CONTENTS

Board of Examiners	ii
Candidate's Declaration	iii
Table of Contents	iv
List of Figurers	vii
List of Tables	x
List of Abbreviations	xi
List of Symbol	xii
Acknowledgement	xiii
Abstract	xiv
Chapter 1: INTRODUCTION	1
1.1 COMMUNICATION SYSTEM	1
1.2 EVOLUTION OF OPTICAL COMMUNICATION	2
1.3 REVIEW OF PREVIOUS WORK	4
1.4 OBJECTIVES OF THE THESIS	7
1.5 THESIS ORGANIZATION	7
Chapter 2: OPTICAL COMMUNICATION AND FIBER NONLINEARITIES	8
2.1 PRINCIPLES OF OPTICAL COMMUNICATION	8
2.1.1 Optical Transmitter	9
2.1.2 Optical Receiver	9
2.1.3 Optical Fiber	10
2.2 OPTICAL FIBER CHARACTERISTICS	10
2.2.1 Linear Characteristics	10
2.2.1.1 Attenuation	11
2.2.1.2 Intrinsic Attenuation	12
2.2.1.2.1. Material Absorption	12
2.2.1.3.2. Rayleigh Scattering	13

2.2.1.3. Extrinsic Attenuation	13
2.2.2.4. Chromatic Dispersion	14
2.3 FIBER TYPES	16
2.3.1 Multimode Fiber with a 50-Micron Core (ITU-T G.651)	16
2.3.2 Non dispersion-Shifted Fiber (ITU-T G.652)	16
2.3.3 1550-nm Loss-Minimized Fiber (ITU-T G.654)	17
2.3.4 Nonzero Dispersion Shifted Fiber (ITU-T G.655)	17
2.3.5 1550-nm Loss-Minimized Fiber (ITU-T G.654)	17
2.3.6 Nonzero Dispersion Shifted Fiber (ITU-T G.655)	17
2.4 WAVELENGTH DIVISION MULTIPLEXING (WDM)	18
2.5 FUNDAMENTALS OF NONLINEAR EFFECTS IN OPTICAL FIBERS	19
2.5.1. Nonlinear Characteristics	19
2.5.1. 1 Stimulated Brillouin Scattering (SBS)	19
2.5.1.2. Stimulated Raman Scattering (SRS)	20
2.5.1.3. Optical Kerr Effect	20
2.5.1.3.1. Self-Phase Modulation (SPM)	20
2.5.1.3.2. Cross- Phase Modulation (XPM)	21
2.5.1.3.3. Four-Wave Mixing (FWM)	22
2.6 SUMMARY	25
Chapter 3:ANALYTICAL MODEL	26
3.1 INTRODUCTION	26
3.2 SYSTEM MODEL	26
3.3 FWM SUPPRESSION MODEL	27
3.4 BIT ERROR RATE (BER)	31
3.5 NOISES IN OPTICAL RECEIVER	33
3.5.1 Thermal noise	33
3.5.2 Shot noise	34
3.5.3 Expression of BER on FWM	34
3.6 SIMULATION SETUP AND DESCRIPTION	35

Chapter 4:RESULT AND DISCUSSION	37
4.1 INTRODUCTION	37
4.2 CROSSTALK EFFECT IN SSMF	37
4.3 CROSSTALK EFFECT IN DSF	41
4.4 CROSSTALK PRESENCE IN LEAF	44
4.5 FWM EFFECT ON ALL KIND OF OPTICAL FIBER	47
4.6 FWM EFFECT ON BIT ERROR RATE (BER)	49
4.7 SIMULATION RESULTS	50
4.8 INPUT/OUTPUT SPECTRUM	50
4.9 FWM EFFECT ON WDM TRANSMISSION SYSTEM	52
4.10 COMPARISON WITH THE PUBLISHED WORKS	55
4.11 DISCUSSION	58
Chapter 5:CONCLUSION AND FUTURE WORK	59
5.1 CONCLUSION	59
5.2 RECOMMENDATIONS FOR FUTURE WORK	60
REFERENCES	61
OUTCOMES OF THIS THESIS WORK	63

LIST OF FIGURES

Figure 2.1	Basic block diagram of an optical fiber communication system.	8
Figure 2.2	Block diagram of an optical transmitter.	9
Figure 2.3	Block diagram of an optical receiver.	10
Figure 2.4	Attenuation v/s wavelength of the fiber.	11
Figure 2.5	Chromatic dispersion parameters in ps/(nm.km) of a standard single-mode fiber as a function of wavelength in nm.	15
Figure 2.6	Graphical Representation of a Point to Point WDM Optical system.	18
Figure 2.7	Phenomenological description of spectral broadening of pulse.	21
Figure 2.8	Four-wave mixing with three injected waves at frequencies f_i, f_j and f_k . The generated frequencies f_{ijk} .	23
Figure 2.9	FWM products calculation as a function of Channel Numbers.	24
Figure 3.1	Block diagram of a WDM system with EDFA in cascade	27
Figure 3.2	Bit error probabilities.	32
Figure 3.3	Simulation of 3-channel WDM system.	35
Figure 4.1	FWM crosstalk as a function of channel input power. Where $D_c = 17\text{ps/km-nm}^2$, $\alpha = 0.25\text{dBm/km}$, $n_2 = 2.65 \times 10^{-20} \text{ m}^2/\text{w}$, $\Delta\lambda = 0.8 \text{ nm}$.	38
Figure 4.2	FWM crosstalk as a function of fiber length. Where $D_c = 17\text{ps/km-nm}^2$, $\alpha = 0.25\text{dBm/km}$, $n_2 = 2.65 \times 10^{-20} \text{ m}^2/\text{w}$, $\Delta\lambda = 0.8 \text{ nm}$, $A_{eff} = 8.8 \mu\text{m}^2$.	39
Figure 4.3	FWM crosstalk as a function of channel spacing. Where $D_c = 17\text{ps/km-nm}^2$, $\alpha = 0.25\text{dBm/km}$, $n_2 = 2.65 \times 10^{-20} \text{ m}^2/\text{w}$, $L = 100\text{km}$.	39
Figure 4.4	FWM crosstalk as a function of dispersion. Where $L = 100\text{km}$, $\alpha = 0.25 \text{ dBm/km}$, $n_2 = 2.65 \times 10^{-20} \text{ m}^2/\text{w}$, $\Delta\lambda = 0.8 \text{ nm}$.	40
Figure 4.5	FWM crosstalk as a function of effective area. Where $L = 100\text{km}$, $\alpha = 0.25 \text{ dBm/km}$, $n_2 = 2.65 \times 10^{-20} \text{ m}^2/\text{w}$, $\Delta\lambda = 0.8 \text{ nm}$.	40
Figure 4.6	FWM crosstalk as a function of channel input power. Where $D_c = 3.5 \text{ ps/km-nm}^2$, $\alpha = 0.25\text{dBm/km}$, $n_2 = 2.65 \times 10^{-20} \text{ m}^2/\text{w}$, $\Delta\lambda = 0.8 \text{ nm}$.	41
Figure 4.7	FWM crosstalk as a function of fiber length. Where $D_c = 3.5\text{ps/km-nm}^2$, $\alpha = 0.25\text{dBm/km}$, $n_2 = 2.65 \times 10^{-20} \text{ m}^2/\text{w}$, $\Delta\lambda = 0.8 \text{ nm}$, $A_{eff} = 5.5 \mu\text{m}^2$.	42

Figure 4.8	FWM crosstalk as a function of channel spacing. Where $D_c = 3.5\text{ps/km-nm}^2$, $\alpha = 0.25\text{dBm/km}$, $n_2 = 2.65 \times 10^{-20} \text{ m}^2/\text{w}$, $L = 100\text{km}$.	42
Figure 4.9	FWM crosstalk as a function of dispersion. Where $L = 100\text{km}$, $\alpha = 0.25\text{dBm/km}$, $n_2 = 2.65 \times 10^{-20} \text{ m}^2/\text{w}$, $\Delta\lambda = 0.8 \text{ nm}$.	43
Figure 4.10	FWM crosstalk as a function of effective area. Where $L = 100\text{km}$, $\alpha = 0.25\text{dBm/km}$, $n_2 = 2.65 \times 10^{-20} \text{ m}^2/\text{w}$, $\Delta\lambda = 0.8 \text{ nm}$.	43
Figure 4.11	FWM crosstalk as a function of channel input power. Where $D_c = 4.5 \text{ ps/km-nm}^2$, $\alpha = 0.25\text{dBm/km}$, $n_2 = 2.65 \times 10^{-20} \text{ m}^2/\text{w}$, $\Delta\lambda = 0.8 \text{ nm}$.	44
Figure 4.12	FWM crosstalk as a function of fiber length. Where $D_c = 4.5\text{ps/km-nm}^2$, $\alpha = 0.25\text{dBm/km}$, $n_2 = 2.65 \times 10^{-20} \text{ m}^2/\text{w}$, $\Delta\lambda = 1.6\text{nm}$, $A_{eff} = 7.2 \mu\text{m}^2$.	45
Figure 4.13	FWM crosstalk as a function of channel spacing. Where $D_c = 4.5\text{ps/km-nm}^2$, $\alpha = 0.25\text{dBm/km}$, $n_2 = 2.65 \times 10^{-20} \text{ m}^2/\text{w}$, $L = 100\text{km}$.	45
Figure 4.14	FWM crosstalk as a function of dispersion. Where $L = 100\text{km}$, $\alpha = 0.25\text{dBm/km}$, $n_2 = 2.65 \times 10^{-20} \text{ m}^2/\text{w}$, $\Delta\lambda = 0.8 \text{ nm}$.	46
Figure 4.15	FWM crosstalk as a function of effective area. Where $L = 100\text{km}$, $\alpha = 0.25\text{dBm/km}$, $n_2 = 2.65 \times 10^{-20} \text{ m}^2/\text{w}$, $\Delta\lambda = 0.8 \text{ nm}$.	46
Figure 4.16	FWM crosstalk as a function of channel input power. Where $L = 100\text{km}$, $\alpha = 0.25\text{dBm/km}$, $n_2 = 2.65 \times 10^{-20} \text{ m}^2/\text{w}$, $\Delta\lambda = 0.8 \text{ nm}$.	47
Figure 4.17	FWM crosstalk as a function of channel spacing. Where $L = 100\text{km}$, $\alpha = 0.25\text{dBm/km}$, $n_2 = 2.65 \times 10^{-20} \text{ m}^2/\text{w}$, $\Delta\lambda = 10.8 \text{ nm}$.	48
Figure 4.18	FWM crosstalk as a function of dispersion. Where $L = 100\text{km}$, $\alpha = 0.25\text{dBm/km}$, $n_2 = 2.65 \times 10^{-20} \text{ m}^2/\text{w}$, $\Delta\lambda = 0.8 \text{ nm}$.	48
Figure 4.19	FWM crosstalk as a function of effective area. Where $L = 100\text{km}$, $\alpha = 0.25\text{dBm/km}$, $n_2 = 2.65 \times 10^{-20} \text{ m}^2/\text{w}$, $\Delta\lambda = 0.8 \text{ nm}$.	49
Figure 4.20	FWM effect on Bit Error rate (BER) in dB. Where $L = 100\text{km}$, $\alpha = 0.25 \text{ dBm/km}$, $n_2 = 2.65 \times 10^{-20} \text{ m}^2/\text{w}$, noise bandwidth, $B = 0.35e^{-9}$, receiver sensitivity, $R_d = 0.8$.	50
Figure 4.21	Pump and probe optical spectrum at the input for 3-channel WDM system	51
Figure 4.22	Pump and probe optical spectrum at the output for 3-channel WDM system	51
Figure 4.23	FWM power Vs channel spacing	52

Figure 4.24	FWM power Vs fiber length	53
Figure 4.25	FWM power Vs Dispersion	53
Figure 4.26	FWM power Vs Effective area	54
Figure 4.27	Calculation of BER on FWM	54
Figure 4.28	Comparison of FWM power versus channel spacing with simulation result	57
Figure 4.29	Comparison of FWM power versus Dispersion with simulation result	58
Figure 4.30	Comparison of FWM power versus effective area with simulation result	58
Figure 4.31	FWM signal against dispersion for equal spaced channel on comprehensive model	59
Figure 4.32	FWM signal against dispersion for equal spaced channel in compared paper [28]	59
Figure 4.33	FWM signal against core effective area for equal spaced channel on comprehensive model	60
Figure 4.34	FWM signal against core effective area for equal spaced channel in compared paper [28]	60
Figure 4.35	FWM power versus input channel power at different values of core effective area under the effect of only β_3 on comprehensive model	60
Figure 4.36	FWM power versus input channel power at different values of core effective area under the effect of only β_3 in compared paper [25]	60
Figure 4.37	Relation curves of FWM power and pump power on comprehensive model	61
Figure 4.38	Relation curves of FWM power and pump power in compared paper [26]	61
Figure 4.39	FWM power and effective core area on comprehensive model	61
Figure 4.40	FWM power and effective core area in compared paper [26]	61

LIST OF TABLES

Table 2.1	Comparison of fiber nonlinearities.	24
Table 4.1	Different system parameters.	37
Table 4.2	Comparison among different related research works.	62

LIST OF ABBREVIATIONS

A = Pulse amplitude

BER = Bit Error Rate

DCF = Dispersion Compensating Fiber

$DWDM$ = Dense Wavelength Division Multiplexing

$EDFA$ = Erbium-Doped Fiber Amplifier

F = Frequency [GHz]

FBG = Fiber Bragg Grating

FWM = Four-Wave Mixing

GVD = Group Velocity Dispersion

L = Fiber length [km]

n = Refractive index

n_2 = Refractive index of the cladding

NRZ = Non-Return-to-Zero bit format

P = Power average in single channel [dBm] or [mW]

PMD = Polarisation Mode Dispersion

Q = Q-factor

R = Resistance [Ω]

RZ = Return-to-Zero bit format

SBS = Stimulated Brillouin Scattering

SNR = Signal-to-Noise Ratio

SMF = Single-Mode Fibre

SPM = Self-Phase Modulation

SRS = Stimulated Raman Scattering

WDM = Wavelength Division Multiplexing

XPM = Cross-Phase Modulation

LIST OF SYMBOL

n	Refractive index
n_2	Nonlinear Refractive index of cladding
c	Velocity of light
	Propagation constant
	Wavelength of light
D	Dispersion
A_{eff}	Effective area
L	Fiber length
	Angular frequency
P_i	Optical input power
P_o	Optical output power
α	Propagation constant
	Permeability
D_c	Chromatic dispersion
P_{FWM}	FWM power
G	Degeneracy factor
γ	Nonlinear coefficient
$\Delta\beta$	Phase matching coefficient
f_{ijk}	Frequency of light
Δf_{ijk}	Channel spacing
L_{eff}	Effective length of fiber
$A_j(z)$	complex electric field envelops
\emptyset_0	Initial phase of the light waves
σ	Noise variance
k	Boltzmann's constant
T	Absolute temperature
B	Post detection bandwidth of the system

ACKNOWLEDGEMENTS

First and foremost I offer my sincerest gratitude to the Almighty Allah for guiding us to conceptualize, develop and complete the thesis. Also this research project would not have been possible without the support of many people. It is a pleasure to convey my gratitude and humble acknowledgement to all of them.

In the first place I want to express special thanks and deepest gratitude to Prof .Dr. Md. Saiful Islam of IICT, BUET for his all advice, guidance and suggestions. Above all and the most needed, he provided me high-spirited encouragement and support in various ways to complete this research work.

I am pleased to thank Professor Dr. Subrata Kumar Aditya , Dept. of Applied Physics, Electronics and Communication Engineering, University of Dhaka for his help and advice, despite of his tight schedules.

I would also like to thank my family members, specially my wife, Suhana Parvin Shuvraand my son Roudroneel Mamun for supporting and encouraging me to pursue this degree.

ABSTRACT

Fiber nonlinearity can cause interactions and severe crosstalk among co-propagating wavelength division multiplexing (WDM) channels in high capacity optical fiber communication system. The crosstalk between channels leads to degradation of the bit error performance of the transmission system. One of the mechanism of this crosstalk is four wave mixing (FWM) caused by the fiber nonlinearity. From different research outcome it is reported that FWM strongly depends on channel spacing, input power, dispersion and core effective area of the fiber. It is essential to evaluate the effect and actual performance degradation due to FWM crosstalk as large amount of optical power is carried by the modern high bit rate WDM channels in long haul communication system. In this research work, a comprehensive analytical model has been developed for evaluation and suppression of FWM effect in a multi-channel fiber-optic transmission system. Using the developed model, FWM suppression performance is evaluated in terms of crosstalk power for 3-different types of communication grade fiber. Through investigation it is found that the amount of FWM crosstalk is lowest in standard single mode fiber (SSMF) than the dispersion shifted fiber (DSF) or large effective area fiber (LEAF). FWM crosstalk also decreases as the channel spacing or effective area increases. Input power and fiber link length also plays a significant role in FWM crosstalk generation. From the analysis and performance evaluation it can be inferred that FWM crosstalk can be minimized by carefully choosing different system design parameters of fiber for high bit rate transmission system.

CHAPTER 1

Introduction

1.1 Communication System

Since the mid 90's, optical fibers have been used for point to point communication at a very high speed. Fiber-optic communication is a method of transmitting information from one place to another by sending light through an optical fiber. Fiber-optic communication systems have revolutionized the telecommunications industry and played a major role in the advent of the information age. Optical fiber offers much higher speed than the speed of electronic signal processing at both ends of the fiber. Because of its advantages over electrical transmission, the use of optical fiber has fully replaced copper wire communications in the developed world. The main benefits of fiber are its exceptionally low loss, allowing long distances between amplifiers or repeaters and its inherently high data-carrying capacity, such that thousands of electrical links would be required to replace a single high bandwidth fiber. Another benefit of fiber is that even when run alongside each other for long distances, fiber cables experience effectively no crosstalk, in contrast to some types of electrical transmission lines.

The main advantages of the optical fiber communications are the high speed, large capacity and high reliability by the use of the broadband of the optical fiber. The huge bandwidth of optical fiber communication system can be utilized to its maximum by using multiple access techniques. So to be able to take the full advantage of the speed in optical fibers one of the basic concepts in fiber optic communication is the idea of allowing several users to transmit data simultaneously over the communication channel by simultaneously allocating the available bandwidth to each user. This is called multiple access. There are two types of multiple access techniques: Asynchronous and Synchronous. Asynchronous multiple access methods, where network access is random and collisions occur are well suited to LAN's with low traffic demand [1]. However, these asynchronous access methods suffer from cumulative delay as the traffic intensity increases. On the other hand, synchronous accessing methods, where transmissions are perfectly scheduled provide more successful transmissions than asynchronous methods [2].

Focus on development of broadband communication systems is incredible since fiber offers combination of wide bandwidth and low losses unmatched by any other transmission medium but group velocity dispersion [3]-[5] and fiber nonlinearities due to optical Kerr's effects [3],[6] remain

inherent limitations of such systems thereby degrading the performance. The progress towards longer lengths of transmission has led to increasing input power and at higher power, nonlinear effect is introduced in the optical fiber that in turn also limits the transmission distance of optical signal [3],[7]. In late 1990s wavelength division multiplexing (WDM) systems have been widely deployed as a solution for higher bit rate transmission. With the increasing demands on the capacity of WDM systems, crosstalk due to nonlinearity become important and FWM is one of the most significant nonlinear effects that impact the system performance [8]-[9]. In the past one decade a number of research works has been carried out on fiber dispersion, nonlinearity and particularly on FWM by analysis, simulation and/ or experimentation [10]- [11].

1.2 Evolution of Optical Communication

Even though an optical communication system had been conceived in the late 18th century by a French Engineer Claude Chappe who constructed an optical telegraph, electrical communication systems remained the dominant means of communication. In 1966, Kao and Hockham proposed the use of optical fiber as a guiding medium for the optical signal [12]. Four years later, a major breakthrough occurred when the fiber loss was reduced to about 20 dB/km from previous values of more than 1000dB/km by applying improved fiber manufacture and design techniques. Since that time, optical communication technology has developed rapidly to achieve larger transmission capacity and longer transmission distance. The capacity of transmission has been increased about 100 fold in every 10 years.

There were several major technological breakthroughs during the past two decades to achieve such a rapid development. In 1980, the bit rate used was 45 Mb/s with repeater spacing of 10 km. The multimode fiber was used as the transmission medium and GaAs LED as the source of the system. In 1987 the bit rate was increased to 1.7 Gbps with repeater spacing of 50 km. By 1990 the bit rate was increased to 2.5 Gbps with repeater spacing further increased to 60-70 km. Dispersion shifted fibers are used to minimize the bit error rate and to increase the repeater spacing and the bit rate.

In 1996, the bit rate of the optical transmission system was increased to 5 Gbps. The development of optical amplifiers brought another important breakthrough in optical communication system. Optical amplifiers reduced the associated delay and power requirement of the electronic amplifiers. WDM was also introduced at this time to increase the available bandwidth capacity in terms of the

channels. By 2002, the bit rate of the optical system was increased to 10 Gbps with repeater spacing of 70-80 km. The introduction of the dense-wavelength division multiplexing (DWDM) system increased the channel capacity and the bit rate got increased to 40 Gbps.

The first generation of optical communication was designed with multi-mode fibers and direct band gap GaAs Light emitting diodes (LEDs) which used to operate at the 0.8 μm – 0.9 μm wavelength range. Compared to the typical repeater spacing of coaxial system (~ 1 km), the longer repeater spacing (~ 10 km) was a major motivation. Large modal dispersion of multi-mode fibers and high fiber loss at 0.8 μm ($>5\text{dB/km}$) limited both the transmission distance and bit rate. In the second generation, multi-mode fibers were replaced by single-mode fibers, and the center wavelength of light sources was shifted to 1.3 μm , where optical fibers have minimum dispersion and lower loss of about 0.5 dB/km.

However, there was still a strong demand to increase repeater spacing further, which could be achieved by operating at 1.55 μm where optical fibers have an intrinsic minimum loss around 0.2 dB/km. Larger dispersion in the 1.55 μm window delayed moving to a new generation until dispersion shifted fiber became available. Dispersion shifted fibers reduced the large amount of dispersion in the 1.55 μm window by modifying the index profile of the fibers while keeping the benefit of low loss at the 1.55 μm window. However, growing communication traffic and demand for larger bandwidth per user revealed a significant drawback of electronic regeneration systems. Because all the regenerators are designed to operate at specific data rate and modulation format, all of them needed to be replaced to convert to a higher data rate.

The difficulty of upgradeability has finally been removed by optical amplifiers, which led to a completely new generation of optical communication. An important advance was that an EDFA at 1.55 μm was found to be ideally suited as an amplifying medium for modern fiber optic communication systems. Invention of the EDFA had a profound impact especially on the design of long haul under sea systems. Trans-oceanic systems installed like TAT(Transatlantic Telephone)-12/13 [13] and TPC (Transpacific Crossings)-5 [14] were designed with EDFA's and the transmission distance reaches over 8000 km without electronic repeaters between terminals. The broad gain spectrum (3~4 THz) of an EDFA also makes it practical to implement WDM systems.

It is highly likely that DWDM systems will bring another big leap of transmission capacity of optical communication systems. Some research groups have already demonstrated that it is possible to transmit almost a Tbps bit rate over thousands of kilometers. There are some important experimental results of DWDM systems [15]. In 1999, a channel system was simulated experimentally with bit

rate 20 Gbps. The system could cover 10,000 km with amplifier spacing of 50 km. The signal format used here was of soliton type. Later the number of channels was increased to 32 with 45 km amplifier spacing and the distance covered was 9,300 km. In this system NRZ and soliton type signal format were used.

In 2004, the number of the channels was increased to 64 at the cost of reduced transmission distance of 500 km with 100 km amplifier spacing. However by 2006 the distance could be extended to 7,200 km with 64 channel system and 10 Gbps bit rate at the cost of reduced amplifier spacing of 50 km. In 2010, the bit rate was increased to 40 Gbps at the cost of reduced number of channels of 34 which could cover a distance of 6,380 km. These results indeed show that remarkable achievements have been made in recent years, and let us forecast that optical communication systems in the next generation will have a transmission capacity of a few hundreds of Gbps [3].

1.3 Review of Previous Work

The understanding of nonlinear processes in optical fibers is crucial towards extending the capabilities of modern optical communication systems based on wavelength division multiplexing (WDM), where each communication channel is represented by a unique wavelength. One of the nonlinear processes that limit the information carrying capacity of a WDM system is FWM, which causes cross-talk between neighboring channels and less the bit rate of the channel. This places a lower limit on the wavelength separation between adjacent channels and an upper limit on the input power in each channel.

B. Goebel *et al.* (2008) analysis the calculation of the number of Four Wave mixing (FWM) products [16] in optical multichannel communication system. They investigated that any three channels create new signal components through the nonlinear process of FWM and also calculated the number of these products for each frequency. The significance of their finding can be useful for nonlinear system analysis of multiplexed fiber-optic communication systems.

R S Kaler, *et al.* (2008), illustrated four wave mixing (FWM) through computer simulations. It has been shown that FWM effect can be suppressed by increasing dispersion in the fibre [17]. The FWM signal power decreases with increasing dispersion but the decrease is not same for equal and unequal spacing. The decrease in FWM power is more for unequal spaced channels as compared to equal

spaced channels. Further it has been shown that with increase in effective area of the fibre, the FWM effect can be reduced.

G. kaur et al (2009), investigated through simulation a dense wavelength division multiplexing (DWDM) optical transmission system and concludes that the increase in the number of channels in the system without changing the channel spacing, results in the increase in the BER due to the effect of FWM [18].

R. Randhawa, *et al.* (2009), proposed a channel allocation method based on unequal channel spacing and has the added advantage of maintaining bandwidth efficiency while reducing FWM effects. However, their work does not show the implementation of the EQC algorithm or search algorithm in real WDM system in order to see the complexity of realizing the unequal channel spacing [19].

G. Hussam *et al* (2007), analytically showed that FWM effect can be suppressed using two or more different modulation technique, at the expense of increased complexity [20].

A.V. Ramprasad *et al* (2006), analytically show that unequal channel spacing reduces the crosstalk power of FWM. A method has been formulated [21] and verified by simulation, the suppression of the side tones due to nonlinearity in the optical propagation. They have shown that when the channel spacing is narrow there is more crosstalk power and the increase in the channel spacing will cause constant crosstalk power.

N. M. Saaid (2010), reviewed the nonlinear effects on optical fiber and found some proposed suppression techniques for FWM effect specially unequal channel spacing [22]. He found FWM can be suppressed by several authors using dispersion management, effective core area, channel Spacing.

Ming-Jun Li *et. Al* (2004),” analytically shows that it is found that large mode area single operation is not arbitrarily scalable with the fiber core size as affected by several practical factor non-linear effects [23].

L. Tawade, *et al.* (2006) investigated that the effect of FWM on Bit Error Rate for Duo-binary & binary modulation like NRZ Rectangular at different dispersion value, core effective area of fiber &

channel spacing for 100km long optical communication system[24]. BER got improved with duobinary modulation format & by increasing core effective area which will offer a significant performance benefit in digital systems.

S. Song *et al.* (2007) have shown that the influence of SPM and XPM on the FWM process becomes significant when the transmitted channel powers are large and the fiber dispersion or the channel spacing is small [25]. Consequently, the conventional formula for calculating the phase-matching conditions for FWM produces significant errors by neglecting the SPM and XPM effects. They have derived a new phase-matching factor by including these effects, resulting in an additional power dependent term with very concise form. Both experimental and calculated results show that the new phase-matching factor produces greatly improved estimates of FWM power generation.

Li Wang *et al.* (2009) investigated FWM Output Power Induced by Phase Modulation in optical Fiber Communication[26]. The Four wave mixing (FWM) power with pump light parameters in standard single-mode fiber, dispersion-shifted fiber, non-zero dispersion fiber and two kinds of dispersion compensating fibers have been compared through numerical simulated calculations. The effect of pump wavelength deduced to the phase-mismatching factor, pump wavelength, pump power and propagation distance to parametric gain and power of FWM have been analyzed in a self-phase modulation and cross-phase modulation. The effect of the pump power, propagation distance and fiber effective core area to FWM have been obtained. It is useful to select the category of fiber and pump, signal wavelength in communication system devices.

From previous works we have found that—

- i) Most of the works are carried out to find the FWM effect on channel Spacing for standard fiber.
- ii) A few works is done considering high order dispersion and core effective area with limited design parameters.
- iii) Still the effect of FWM for WDM transmission system of DSF, SSMF and LEAF on dispersion, core effective area is unexplored using a comprehensive model of suppressing FWM with all system parameters like- channel spacing, input power, dispersion and core effective area.

After reviewing all the papers it is observed that FWM has immense effect for decreasing the bit rate of the fiber. All the researchers are focusing on the channel spacing parameters for decreasing the FWM effect with fixed model for the other system parameters. But it is also found that some works have proposed some model for suppressing FWM by modulation technique but there is no common or comprehensive model design for WDM which can be used for suppressing and analyzing for FWM effect with all system parameters that may have great impact on FWM and all of the researchers are concluded their works considering a standard optical fiber parameters values but it is not yet explored that which kind of manufactured fiber has less effect of FWM for higher data transmission for long haul WDM communication.

1.4 Objectives of the Thesis

Transmission in WDM optical fiber communication system is mainly impaired and ultimately limited by FWM. FWM is a nonlinear phenomenon in optical fibers only when two or more optical fields are transmitted through the fiber simultaneously. The effect of FWM become prominent and it also need to be considered at high bit rate optical transmission system. The main objectives of this research work are:

- (i) To derive an analytical model for studying the effect of FWM
- (ii) To find the effect of channel spacing as function of modulation frequency due to FWM,
- (iii) To find the effect of dispersion and effective area as function of modulation frequency due to FWM,
- (iv) To compare the above mentioned effects with simulated result.

1.5 Thesis Organization

In chapter 2 we focus on basic of optical fibers and its properties, where we discuss briefly about impairments, linear effects and nonlinear effects. In chapter 3 we discuss about analytical model for FWM and its derivation. In chapter 4 we present the results and discussion. In Chapter 5 brings the conclusion of the total analysis and discuss about the further field of research.

1.6 Summery

In this chapter briefly discuss the evolution of fiber optics communication and also discuss the previous works done by the other researchers. Also, mentioned the motivation and synopsis of the thesis works.

CHAPTER 2

Optical Communication and Fiber Nonlinearities

2.1 Principles of Optical Communication

An optical fiber communication system is a particular type of telecommunication system, in which information to be conveyed enters an electronic transmitter, where it is prepared for transmission very much in the conventional manner. The signal then moves to the optical transmitter, where it is converted into optical form and the resulting light signal is transmitted over optical fiber. At the receiver end, an optical detector converts the light back into an electrical signal, which is processed by the electronic receiver to extract the information and present it in a usable form (audio, video, or data output). So a typical optical communication system consists of three major components: optical transmitter, optical fiber and optical receiver as in Fig. 2.1.

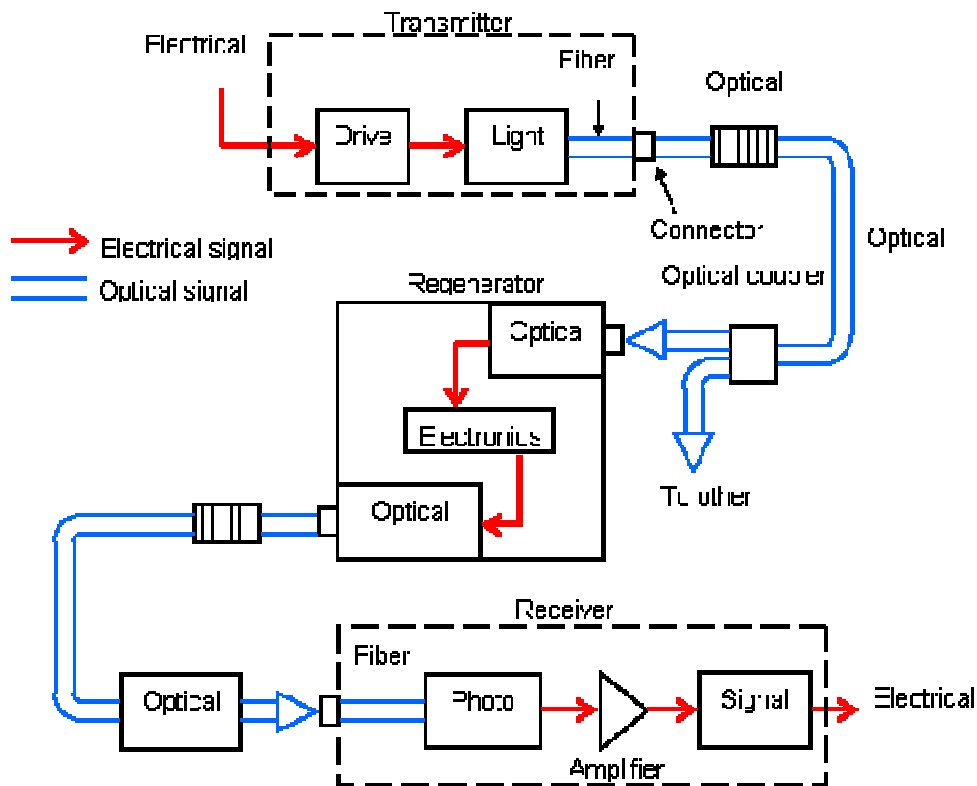


Fig 2.1: Basic block diagram of an optical fiber communication system

2.1.1 Optical Transmitter

The heart of the optical transmitter is a light source. The main function of an optical transmitter is to transform the electrical signal into optical signal using light source. The block diagram of an optical transmitter is shown in Fig 2.2. It consists of an optical source, a modulator and a channel coupler. Semiconductor laser or light emitting diodes are used as optical source. The main consideration in selecting a source is its ability in launching maximum power into the optical fiber in suitable wavelength. The optical signal is generated after modulating the light wave by the input signal. The coupler is generally a micro-lens that focuses the optical signal onto the entrance plane of an optical fiber with the maximum possible efficiency. The amount of launched power is an important factor in designing the optical communication system.

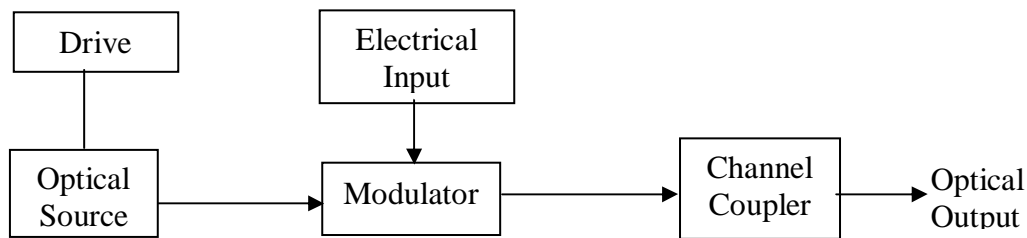


Fig 2.2: Block diagram of an optical transmitter

2.1.2 Optical Receiver

The key component of an optical receiver is its photo-detector. The main function of optical receiver is to convert the received optical signal from the fiber into the original electrical signal using photo-detector. The block diagram of an optical receiver is shown in Fig 2.3. The optical receiver specially consists of a coupler, a photo-detector, and a demodulator. The coupler focuses the received optical signal onto the photo-detector. Semiconductor photo diodes are used as photo-detectors because of their compatibility with the whole system. The design of the modulator depends on the modulation format used in the system. The design of the modulator depends on the modulation format used in the system. One of the most important design parameter is receiver sensitivity.

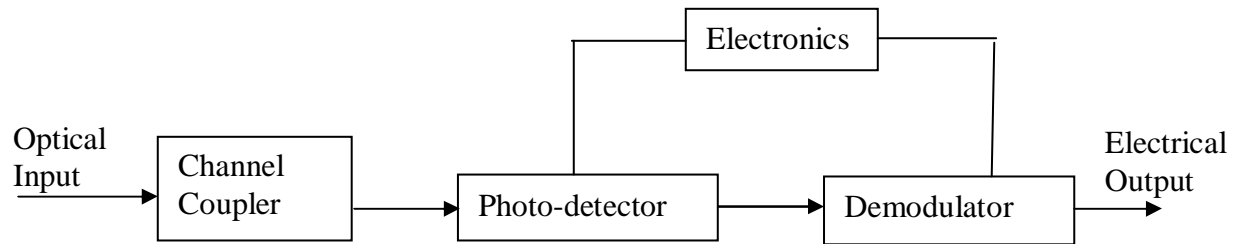


Fig 2.3: Block diagram of an optical receiver

2.1.3 Optical Fiber

Optical fiber is the transmission medium of the optical fiber communication system which bridge the distance between the optical transmitter and the optical receiver. To ensure the propagation of the transmitted signal up to the receiver with acceptable level of attenuation and distortion is the main consideration in designing the fiber so that the same information can be received at the receiver with minimum error. With the development in the field of optical fiber communication, the attenuation of the signal could be reduced to 0.2 dB/km. Factors that contributed to this reduction in the loss parameter are improved fiber design technique, low loss fiber window, dispersion compensation, etc [3]. Fiber loss, dispersion and nonlinear effects are main design considerations of optical fiber. Introduction of optical amplifiers and dispersion shifted fibers could successfully address the limitations imposed by fiber loss and dispersion. But many aspects of nonlinear characteristics of the fiber yet remained as the limitation of optical fibers.

2.2 Optical Fiber Characteristics

Optical fiber systems have many advantages over metallic based communication systems. These advantages include interference, attenuation, and bandwidth characteristics. Furthermore, the relatively smaller cross section of fiber-optic cables allows room for substantial growth of the capacity in existing conduits. Fiber-optic characteristics can be classified as linear and nonlinear. Nonlinear characteristics are influenced by parameters, such as bit rates, channel spacing, and power levels.

2.2.1 Linear Characteristics

Linear characteristics include attenuation, chromatic dispersion (CD), polarization mode dispersion (PMD), and optical signal-to-noise ratio (OSNR).

2.2.1.1 Attenuation

Several factors can cause attenuation, but it is generally categorized as either intrinsic or extrinsic. Intrinsic attenuation is caused by substances inherently present in the fiber, whereas extrinsic attenuation is caused by external forces such as bending. The attenuation coefficient α is expressed in decibels per kilometer and represents the loss in decibels per kilometer of fiber. Attenuation characteristics are shown in Fig. 2.4.

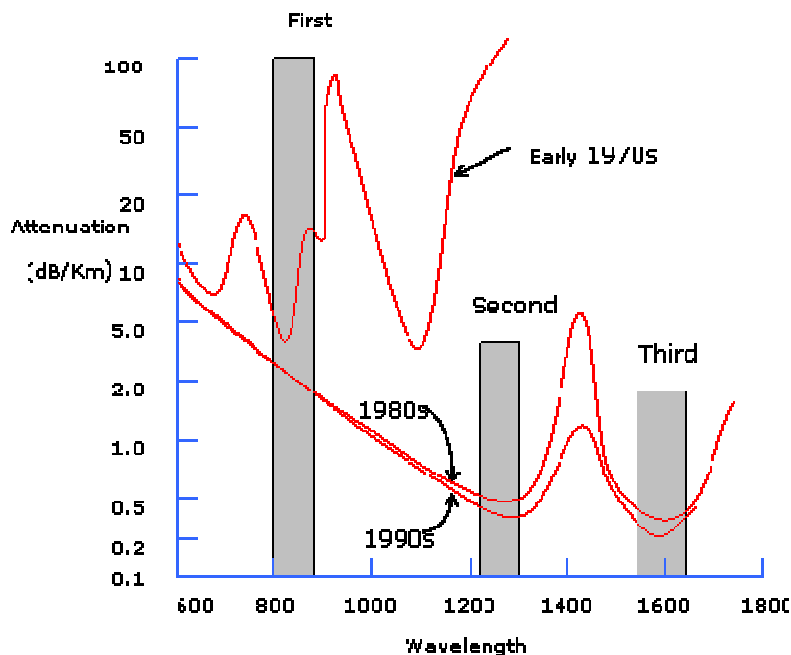


Fig. 2.4: Attenuation v/s wavelength of the fiber.

An important fiber parameter is the measure of power loss during transmission of optical signals inside an optical fiber. If P_0 is the power launched at the input of a fiber of length L , the transmitted power P_T is given by

$$P_T = P_0 \exp(-\alpha L), \quad (2.1)$$

Where the attenuation coefficient α is a measure of overall fiber losses from all sources. It is customary to express α in units of dB/km by the relation

$$[dB/km] = -\frac{10}{L} \text{Log}_{10} \left(\frac{P_{out}}{P_{in}} \right) \approx 4.343 \quad (2.2)$$

Several intrinsic and extrinsic sources contribute to the overall losses; the most important among them is Rayleigh scattering. Rayleigh scattering is the fundamental loss in optical fiber. It is referred to scattering is the fundamental loss in optical fiber. It is referred to scattering of light by random fluctuations in refractive index on a scale smaller than the optical wavelength. The loss is expressed in dB/km through

$$\alpha_R = C / \lambda^4 \quad (2.3)$$

Where C is a constant. Rayleigh scattering varies as a function of λ^{-4} and is the dominant loss mechanism for wavelengths shorter than 1.2 μm . The attenuation of a standard step-index single-mode fiber is about 12 dB/km near 630 nm.

2.2.1.2 Intrinsic Attenuation

Intrinsic attenuation results from materials inherent to the fiber. It is caused by impurities in the glass during the manufacturing process. As precise as manufacturing is, there is no way to eliminate all impurities. When a light signal hits an impurity in the fiber, one of two things occurs: It scatters or it is absorbed. Intrinsic loss can be further characterized by two components:

- Material absorption
- Rayleigh scattering

2.2.1.2.1 Material Absorption

Material absorption occurs as a result of the imperfection and impurities in the fiber. The most common impurity is the hydroxyl (OH-) molecule, which remains as a residue despite stringent manufacturing techniques. Figure 3-12 shows the variation of attenuation with wavelength measured over a group of fiber-optic cable material types. The three principal windows of operation include the 850-nm, 1310-nm, and 1550-nm wavelength bands. These correspond to wavelength regions in which attenuation is low and matched to the capability of a transmitter to generate light efficiently and a receiver to carry out detection. The OH- symbols indicate that at the 950-nm, 1380-nm, and

2730-nm wavelengths, the presence of hydroxyl radicals in the cable material causes an increase in attenuation. These radicals result from the presence of water remnants that enter the fiber-optic cable material through either a chemical reaction in the manufacturing process or as humidity in the environment. The variation of attenuation with wavelength due to the *water peak* for standard, single-mode fiber-optic cable occurs mainly around 1380 nm. Recent advances in manufacturing have overcome the 1380-nm water peak and have resulted in zero-water-peak fiber (ZWPF). Examples of these fibers include SMF-28e from Corning and the Furukawa-Lucent OFS AllWave. Absorption accounts for three percent to five percent of fiber attenuation. This phenomenon causes a light signal to be absorbed by natural impurities in the glass and converted to vibration energy or some other form of energy such as heat. Unlike scattering, absorption can be limited by controlling the amount of impurities during the manufacturing process. Because most fiber is extremely pure, the fiber does not heat up because of absorption.

2.2.1.2.2 Rayleigh Scattering

As light travels in the core, it interacts with the silica molecules in the core. Rayleigh scattering is the result of these elastic collisions between the light wave and the silica molecules in the fiber. Rayleigh scattering accounts for about 96 percent of attenuation in optical fiber. If the scattered light maintains an angle that supports forward travel within the core, no attenuation occurs. If the light is scattered at an angle that does not support continued forward travel, however, the light is diverted out of the core and attenuation occurs. Depending on the incident angle, some portion of the light propagates forward and the other part deviates out of the propagation path and escapes from the fiber core. Some scattered light is reflected back toward the light source. This is a property that is used in an optical time domain reflectometer (OTDR) to test fibers. The same principle applies to analyzing loss associated with localized events in the fiber, such as splices.

Short wavelengths are scattered more than longer wavelengths. Any wavelength that is below 800 nm is unusable for optical communication because attenuation due to Rayleigh scattering is high. At the same time, propagation above 1700 nm is not possible due to high losses resulting from infrared absorption.

2.2.1.2.3 Extrinsic Attenuation

Extrinsic attenuation can be caused by two external mechanisms: macrobending or microbending. Both cause a reduction of optical power. If a bend is imposed on an optical fiber, strain is placed on

the fiber along the region that is bent. The bending strain affects the refractive index and the critical angle of the light ray in that specific area. As a result, light traveling in the core can refract out, and loss occurs.

A macrobend is a large-scale bend that is visible, and the loss is generally reversible after bends are corrected. To prevent macrobends, all optical fiber has a minimum bend radius specification that should not be exceeded. This is a restriction on how much bend a fiber can withstand before experiencing problems in optical performance or mechanical reliability.

The second extrinsic cause of attenuation is a microbend. Microbending is caused by imperfections in the cylindrical geometry of fiber during the manufacturing process. Microbending might be related to temperature, tensile stress, or crushing force. Like macrobending, microbending causes a reduction of optical power in the glass. Microbending is very localized, and the bend might not be clearly visible on inspection. With bare fiber, microbending can be reversible.

2.2.1.2.4 Chromatic Dispersion

Chromatic dispersion is the spreading of a light pulse as it travels down a fiber. Light has a dual nature and can be considered from an electromagnetic wave as well as quantum perspective. This enables us to quantify it as waves as well as quantum particles. During the propagation of light, all of its spectral components propagate accordingly. These spectral components travel at different group velocities that lead to dispersion called group velocity dispersion (GVD). Dispersion resulting from GVD is termed chromatic dispersion due to its wavelength dependence. The effect of chromatic dispersion is pulse spread.

As the pulses spread, or broaden, they tend to overlap and are no longer distinguishable by the receiver as 0s and 1s. Light pulses launched close together (high data rates) that spread too much (high dispersion) result in errors and loss of information. Chromatic dispersion occurs as a result of the range of wavelengths present in the light source. Light from lasers and LEDs consists of a range of wavelengths, each of which travels at a slightly different speed. Over distance, the varying wavelength speeds cause the light pulse to spread in time. This is of most importance in single-mode applications. Modal dispersion is significant in multimode applications, in which the various modes of light traveling down the fiber arrive at the receiver at different times, causing a spreading effect. Chromatic dispersion is common at all bit rates. Chromatic dispersion can be compensated for or mitigated through the use of dispersion-shifted fiber (DSF). DSF is fiber doped with impurities that

have negative dispersion characteristics. Chromatic dispersion is measured in ps/nm-km. A 1-dB power margin is typically reserved to account for the effects of chromatic dispersion. Dispersion effect on different fiber are shown in Fig. 2.5.

When an electromagnetic wave interacts with bound electrons of a dielectric. The medium response in general depends on the optical frequency ω . This property referred to as chromatic dispersion. The chromatic dispersion parameter in a single mode fiber is the sum of the material and waveguide dispersions, so that:

$$D(\lambda) = D_{\text{mat}}(\lambda) + D_{\text{wg}}(\lambda) \quad (2.4)$$

This relation is very important since the material dispersion parameter above 1300 nm becomes positive while the waveguide dispersion parameter stays negative. The fact is that they cancel each other out, resulting in a zero chromatic – dispersion parameter $D(\lambda) = 0$. This occurs around 1310 nm, the customary operating wave for standard single mode fiber [Figure 2.5]. Pulse spreading caused by chromatic dispersion,

$$\Delta t_{\text{chrom}} / L = D(\lambda) \Delta \quad (2.5)$$

Where $D(\lambda)$ is the chromatic dispersion parameter of the fiber and Δ is the spectral width of the light source, as is customary.

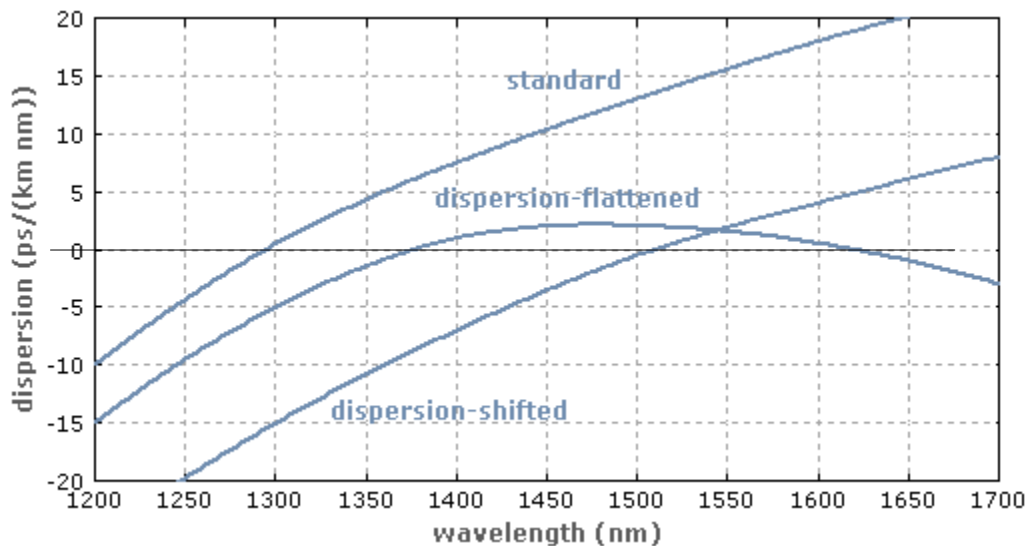


Fig. 2.5: Chromatic dispersion parameters in ps/(nm.km) of a standard single-mode fiber as a function of wavelength in nm.

Manufacturers specify the chromatic –dispersion parameter for multimode fibers either by giving its value or by giving the formula:

$$D(\lambda) = \frac{S_0}{4} \left[-\frac{4}{\lambda^3} \right] \quad (2.6)$$

Where S_0 is the zero-dispersion slope in ps/(nm².km), λ_0 is the zero dispersion wavelength, and λ is the operating wavelength.

To calculate the dispersion parameter near the zero dispersion wavelength, λ_0 , one can use a simplified version of the above formula:

$$D(\lambda) = S_0 \left[\lambda - \lambda_0 \right] \quad (2.7)$$

Where the zero dispersion slope, S_0 can be found in a fiber data sheet.

The dispersion parameter D is commonly used in place of β_2 to describe the total dispersion of a single mode fiber. It is related to β_2 by the relation

$$D = \frac{d\beta_1}{d\lambda} = -\frac{2}{c} \beta_2 \quad (2.8)$$

However, chromatic dispersion is an important phenomenon in the propagation of short pulses in optical fibers. Temporally short pulses have a large spectral bandwidth. The different spectral components of the pulse travel through the medium at slightly different group velocities because of chromatic dispersion, which can result in a temporal broadening of the light pulses with no effect on their spectral compositions. This phenomenon is referred to as group velocity dispersion (GVD).

2.3 Fiber Types

This section discusses various MMF and SMF types currently used for premise, metro, aerial, submarine, and long-haul applications. The International Telecommunication Union (ITU-T), which is a global standardization body for telecommunication systems and vendors, has standardized various fiber types. These include the 50/125 μm graded index fiber (G.651), non-dispersion-shifted fiber (G.652), dispersion-shifted fiber (G.653), 1550-nm loss-minimized fiber (G.654), and NZDSF (G.655).

2.3.1 Multimode Fiber with a 50-Micron Core (ITU-T G.651)

The ITU-T G.651 is an MMF with a 50 μm nominal core diameter and a 125 μm nominal cladding diameter with a graded refractive index. The attenuation parameter for G.651 fiber is typically 0.8

dB/km at 1310 nm. The main application for ITU-T G.651 fiber is for short-reach optical transmission systems. This fiber is optimized for use in the 1300-nm band. It can also operate in the 850-nm band.

2.3.2 Non dispersion-Shifted Fiber (ITU-T G.652)

The ITU-T G.652 fiber is also known as standard SMF and is the most commonly deployed fiber. This fiber has a simple step-index structure and is optimized for operation in the 1310-nm band. It has a zero-dispersion wavelength at 1310 nm and can also operate in the 1550-nm band, but it is not optimized for this region. The typical chromatic dispersion at 1550 nm is high at 17 ps/nm-km. Dispersion compensation must be employed for high-bit-rate applications. The attenuation parameter for G.652 fiber is typically 0.2 dB/km at 1550 nm, and the PMD parameter is less than 0.1 ps/ km. An example of this type of fiber is Corning SMF-28.

2.3.3 Low Water Peak Non-dispersion-Shifted Fiber (ITU-T G.652.C)

The legacy ITU-T G.652 standard SMFs are not optimized for WDM applications due to the high attenuation around the water peak region. ITU G.652.C-compliant fibers offer extremely low attenuation around the OH peaks. The G.652.C fiber is optimized for networks where transmission occurs across a broad range of wavelengths from 1285 nm to 1625 nm. Although G.652.C-compliant fibers offer excellent capabilities for shorter, unamplified metro and access networks, they do not fully address the needs for 1550-nm transmission. The attenuation parameter for G.652 fiber is typically 0.2 dB/km at 1550 nm, and the PMD parameter is less than 0.1 ps/ km. An example of this type of fiber is Corning SMF-28e.

2.3.4 Dispersion-Shifter Fiber (ITU-T G.653)

Conventional SMF has a zero-dispersion wavelength that falls near the 1310-nm window band. SMF shows high dispersion values over the range between 1500 nm and 1600 nm (third window band). The trend of shifting the operating transmission wavelength from 1310 nm to 1550 nm initiated the development of a fiber type called dispersion-shifted fiber (DSF). DSF exhibits a zero-dispersion value around the 1550-nm wavelength where the attenuation has minimum. The DSFs are optimized for operating in the region between 1500 to 1600 nm. With the introduction of WDM systems, however, channels allocated near 1550 nm in DSF are seriously affected by noise induced as a result of nonlinear effects caused by FWM. This initiated the development of NZDSF. Figure 3-14

illustrates the dispersion slope of DSF with respect to SMF and NZDSF. G.53 fiber is rarely deployed anymore and has been superseded by G.655.

2.3.5 1550-nm Loss-Minimized Fiber (ITU-T G.654)

The ITU-T G.654 fiber is optimized for operation in the 1500-nm to 1600-nm region. This fiber has a low loss in the 1550-nm band. Low loss is achieved by using a pure silica core. ITU-T G.654 fibers can handle higher power levels and have a larger core area. These fibers have a high chromatic dispersion at 1550 nm. The ITU G.654 fiber has been designed for extended long-haul undersea applications.

2.3.6 Nonzero Dispersion Shifted Fiber (ITU-T G.655)

Using nonzero dispersion-shifted fiber (NZDSF) can mitigate nonlinear characteristics. NZDSF fiber overcomes these effects by moving the zero-dispersion wavelength outside the 1550-nm operating window. The practical effect of this is to have a small but finite amount of chromatic dispersion at 1550 nm, which minimizes nonlinear effects, such as FWM, SPM, and XPM, which are seen in the dense wavelength-division multiplexed (DWDM) systems without the need for costly dispersion compensation. There are two fiber families called nonzero dispersion (NZD+ and NZD-), in which the zero-dispersion value falls before and after the 1550-nm wavelength, respectively. The typical chromatic dispersion for G.655 fiber at 1550 nm is 4.5 ps/nm-km. The attenuation parameter for G.655 fiber is typically 0.2 dB/km at 1550 nm, and the PMD parameter is less than 0.1 ps/km. The Corning LEAF fiber is an example of an enhanced G.655 fiber with a 32 percent larger effective area.

2.4 Wavelength Division Multiplexing (WDM)

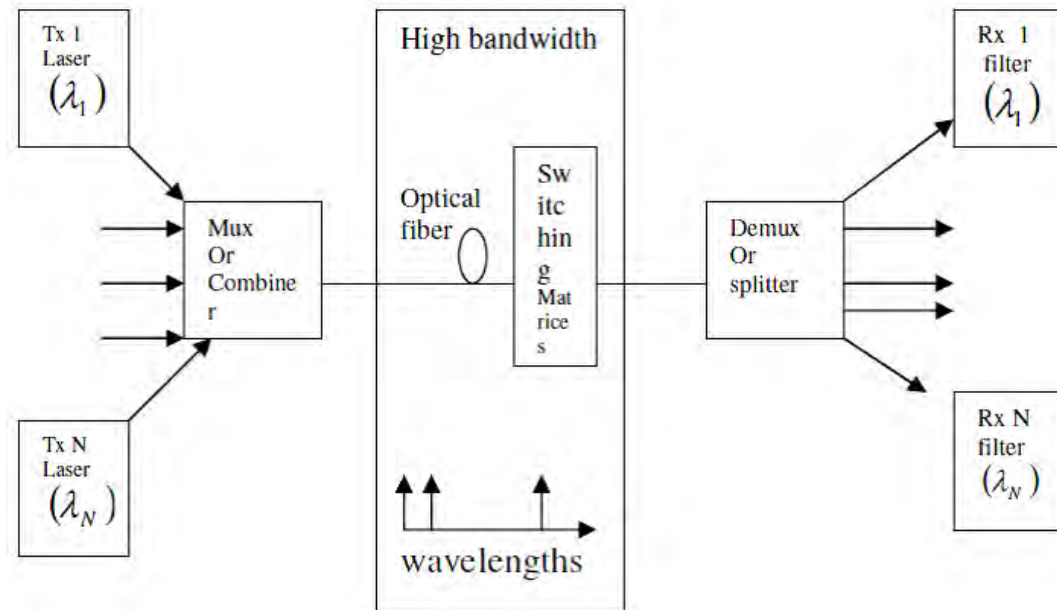


Fig. 2.6: Graphical Representation of a Point to Point WDM Optical system.

A typical first generation long distance WDM configuration, transmission is point-to-point. This is just logically the superposition of many single-channel systems onto a single fiber. It should be noted that each optical channel is completely independent of the other optical channels. It may run at its own rate (speed) and use its own encodings and protocols without any dependence on the other channels at all. All of the current systems use a range of wavelengths between 1540 nm and 1560 nm. There are two reasons for this: First to take advantage of the “low loss” transmission window in optical fiber and second to enable the use of erbium doped fiber amplifiers. Channel speeds for WAN applications are typically 2.4 Gbps in current operational WDM systems. In the figure each channel is shown being electronically multiplexed and de-multiplexed. In many systems this will be true. However, this is just for illustration purposes. There is no requirement for electronic TDM multiplexing. Each channel is just a clear bit stream with its own unique timing and each may be treated in whatever way is appropriate for its particular role.

2.5 Fundamentals of Nonlinear Effects in Optical Fibers

The non-linear effects of the fibers play a detrimental role in the light propagation. Nonlinear Kerr effect is the dependence of refractive index of the fiber on the power that is propagating through it.

This effect is responsible for SPM, XPM and FWM. The other two important effects are stimulated Brillouin scattering (SBS) and stimulated Raman scattering (SRS).

2.5.1 Nonlinear Characteristics

Nonlinear characteristics include self-phase modulation (SPM), cross-phase modulation (XPM), four-wave mixing (FWM), stimulated Raman scattering (SRS), and stimulated Brillouin scattering (SBS).

2.5.2 Stimulated Brillouin Scattering (SBS)

SBS falls under the category of inelastic scattering in which the frequency of the scattered light is shifted downward [4]. This results in the loss of the transmitted power along the fiber. At low power levels, this effect will become negligible. SBS sets a threshold on the transmitted power, above which considerable amount of power is reflected. This back reflection will make the light to reverse direction and travel towards the source. This usually happens at the connector interfaces where there is a change in the refractive index. As the power level increases, more light is backscattered since the level would have crossed the SBS threshold. The parameters which decide the threshold are the wavelength and the line-width of the transmitter. Lower line-width experiences lesser SBS and the increase in the spectral width of the source will reduce SBS. In case of bit streams with shorter pulse width, no SBS will occur [4]. The value of the threshold depends on the RZ and NRZ waveforms which are used to modulate the source. It is typically 5 mW and can be increased to 10 mW by increasing the bandwidth of the carrier greater than 200 MHz by phase modulation [4].

SBS is due to the acoustic properties of photon interaction with the medium. When light propagates through a medium, the photons interact with silica molecules during propagation. The photons also interact with themselves and cause scattering effects such as SBS in the reverse direction of propagation along the fiber. In SBS, a low-wavelength wave called *Stoke's wave* is generated due to the scattering of energy. This wave amplifies the higher wavelengths. The gain obtained by using such a wave forms the basis of Brillouin amplification. The Brillouin gain peaks in a narrow peak near the C-band. SBS is pronounced at high bit rates and high power levels. The margin design requirement to account for SRS/SBS is 0.5 dB.

2.5.3 Stimulated Raman Scattering (SRS)

When light propagates through a medium, the photons interact with silica molecules during propagation. The photons also interact with themselves and cause scattering effects, such as stimulated Raman scattering (SRS), in the forward and reverse directions of propagation along the fiber. This results in a sporadic distribution of energy in a random direction.

SRS refers to lower wavelengths pumping up the amplitude of higher wavelengths, which results in the higher wavelengths suppressing signals from the lower wavelengths. One way to mitigate the effects of SRS is to lower the input power. In SRS, a low-wavelength wave called Stoke's wave is generated due to the scattering of energy. This wave amplifies the higher wavelengths. The gain obtained by using such a wave forms the basis of Raman amplification. The Raman gain can extend most of the operating band (C- and L-band) for WDM networks. SRS is pronounced at high bit rates and high power levels. The margin design requirement to account for SRS/SBS is 0.5 dB.

2.5.4 Optical Kerr Effect

The Kerr effect, also called the quadratic electro-optic effect (QEO effect), is a change in the refractive index of a material in response to an applied electric field. The Kerr effect was discovered in 1875 by John Kerr, a Scottish physicist. The optical Kerr effect, or AC Kerr effect is the case in which the electric field is due to the light itself. This causes a variation in index of refraction which is proportional to the local irradiance of the light. This refractive index variation is responsible for the nonlinear optical effects of self-focusing, self-phase modulation and modulational instability, and is the basis for Kerr-lens modelocking. This effect only becomes significant with very intense beams such as those from lasers.

2.5.3.1. Self-Phase Modulation (SPM)

Phase modulation of an optical signal by itself is known as self-phase modulation (*SPM*). SPM is primarily due to the self-modulation of the pulses. Generally, SPM occurs in single-wavelength systems. At high bit rates, however, SPM tends to cancel dispersion. SPM increases with high signal power levels. In fiber plant design, a strong input signal helps overcome linear attenuation and dispersion losses. However, consideration must be given to receiver saturation and to nonlinear effects such as SPM, which occurs with high signal levels. SPM results in phase shift and a nonlinear pulse spread shown in the Fig. 2.6. As the pulses spread, they tend to overlap and are no

longer distinguishable by the receiver. The acceptable norm in system design to counter the SPM effect is to take into account a power penalty that can be assumed equal to the negative effect posed by XPM. A 0.5-dB power margin is typically reserved to account for the effects of SPM at high bit rates and power levels.

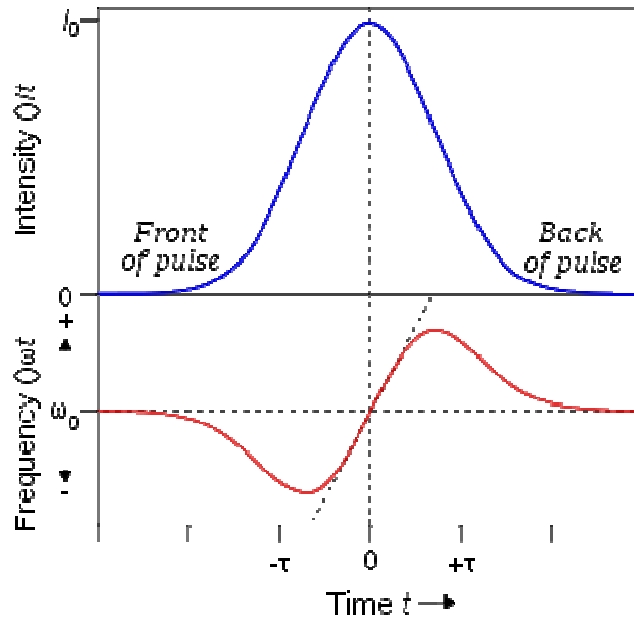


Fig. 2.7: Phenomenological description of spectral broadening of pulse due to SPM.

2.5.3.2. Cross- Phase Modulation (XPM)

Another nonlinear phase shift originating from the Kerr effect is cross-phase modulation (XPM). While SPM is the effect of a pulse on its own phase, XPM is a nonlinear phase effect due to optical pulses in neighboring channels. Therefore, XPM occurs only in multi-channel systems. In a multi-channel system, the nonlinear phase shift of the signal at the center wavelength ω_i is described by [],

$$\phi_{NL} = \frac{2}{i} n_2 z \left[I_i(t) + 2 \sum_{i \neq j}^M I_j(t) \right] \quad (2.9)$$

Where M is the number of co-propagating channels in the fiber. The first term is responsible for SPM, and the second term is for XPM. Equation (2.1) might lead to a speculation that the effect of XPM could be at least twice as significant as that of SPM. XPM is a nonlinear effect that limits system performance in wavelength-division multiplexed (WDM) systems. XPM is the phase modulation of a signal caused by an adjacent signal within the same fiber. XPM is related to the

combination (dispersion/effective area). XPM results from the different carrier frequencies of independent channels, including the associated phase shifts on one another. The induced phase shift is due to the walkover effect, whereby two pulses at different bit rates or with different group velocities walk across each other. As a result, the slower pulse sees the walkover and induces a phase shift. The total phase shift depends on the net power of all the channels and on the bit output of the channels. Maximum phase shift is produced when bits belonging to high-powered adjacent channels walk across each other.

XPM can be mitigated by carefully selecting unequal bit rates for adjacent WDM channels. XPM, in particular, is severe in long-haul WDM networks, and the acceptable norm in system design to counter this effect is to take into account a power penalty that can be assumed equal to the negative effect posed by XPM. A 0.5-dB power margin is typically reserved to account for the effects of XPM in WDM fiber systems.

However, XPM is effective only when pulses in the other channels are synchronized with the signal of interest. When pulses in each channel travel at different group velocities due to dispersion, the pulses slide past each other while propagating. Figure (2.6) illustrates how two isolated pulses in different channels collide with each other. When the faster traveling pulse has completely walked through the slower traveling pulse, the XPM effect becomes negligible. The relative transmission distance for two pulses in different channels to collide with each other is called walk-off distance, L_w [36].

$$L_w = \frac{T_0}{v_g(\lambda_1) - v_g(\lambda_2)} \approx \frac{T_0}{|D\Delta\lambda|} \quad (2.10)$$

where T_0 is the pulse width, v_g is the group velocity, and λ_1, λ_2 are the center wavelength of the two channels. D is the dispersion coefficient and $\Delta\lambda = |\lambda_1 - \lambda_2|$. When dispersion is significant, the walk-off distance is relatively short, and the interaction between the pulses will not be significant, which leads to a reduced effect of XPM. However, the spectrum broadened due to XPM will induce more significant distortion of temporal shape of the pulse when large dispersion is present, which makes the effect of dispersion on XPM complicated.

2.5.3.3. Four-Wave Mixing (FWM)

FWM can be compared to the inter-modulation distortion in standard electrical systems. When three wavelengths (λ_1 , λ_2 , and λ_3) interact in a nonlinear medium, they give rise to a fourth wavelength (λ_4), which is formed by the scattering of the three incident photons, producing the fourth photon. This effect is known as four-wave mixing (FWM) and is a fiber-optic characteristic that affects WDM systems.

The effects of FWM are pronounced with decreased channel spacing of wavelengths and at high signal power levels. High chromatic dispersion also increases FWM effects. FWM also causes inter-channel cross-talk effects for equally spaced WDM channels. FWM can be mitigated by using uneven channel spacing in WDM systems or nonzero dispersion-shifted fiber (NZDSF). A 0.5-dB power margin is typically reserved to account for the effects of FWM in WDM systems.

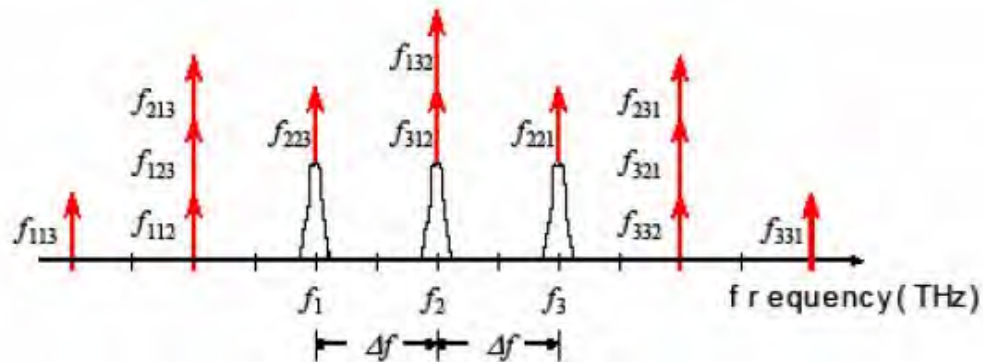


Fig. 2.8: Four-wave mixing with three injected waves at frequencies f_i , f_j and f_k . The generated frequencies f_{ijk}

In WDM system, FWM process can seriously degrade the performances of the system : FWM process with 3 different channels at frequencies f_i, f_j, f_k will generate waves at frequencies $\omega_{ijk} = \omega_i + \omega_j + \omega_k$. If the WDM channels are equally spaced, the FWM products overlap the channel spectra. It is easy to observe the effect of FWM in the time domain since it interferes with the signal coherently. Since the FWM power depends on the bit pattern of the channels, the signal power may fluctuate considerably.

N channels generate $M = \left(\frac{N^3 - N^2}{2} \right)$ products. Where N is the number of channels and M is the number of newly generated side bands. For example, eight (8) channels produce 224 side bands. The Figure 2.5 shows the FWM products due to the channels increase. One solution to reduce the FWM crosstalk is to allocate the channel wavelengths in a non-uniform way so that the FWM component will not fall into the channel spectra.

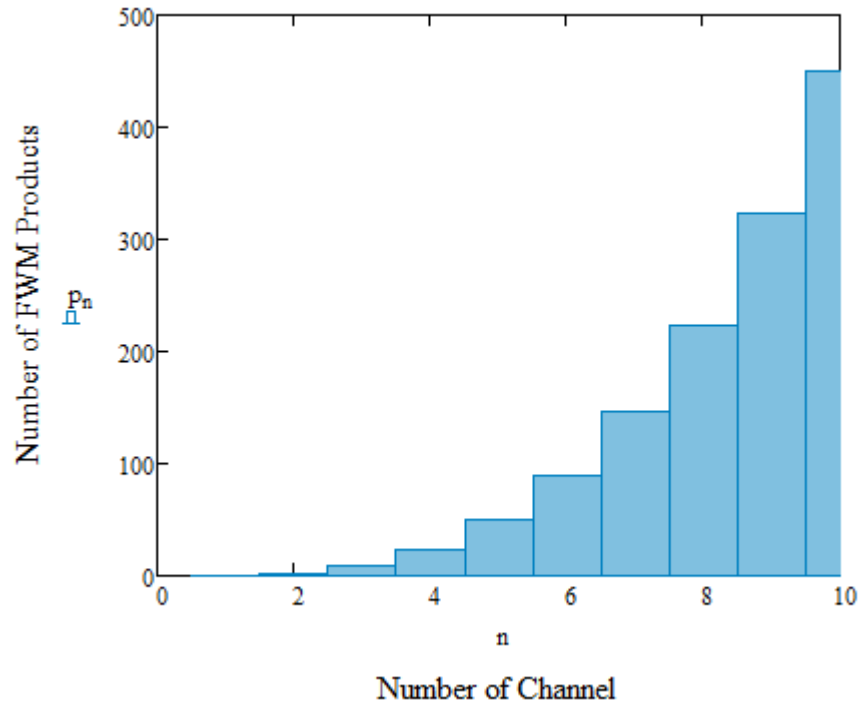


Fig. 2.9: FWM products calculation as a function of Channel Numbers

Table 2.1: Comparison of fiber nonlinearities.

Nonlinear Phenomenon	SPM	XPM	FWM
1. Bit Rate	Dependent	Dependent	Independent
2. Origin	Nonlinear susceptibility	Nonlinear susceptibility	Nonlinear susceptibility
3. Effect of X	Phase shift due pulse itself only	Phase shift is alone due to co-propagating Signal	New waves are generated

4. Shape of Broadening	Symmetrical	May be Symmetrical	-
5. Energy transfer between medium and optical pulse	No	No	No
6. Channel Spacing	No effect	Increases on decreasing the spacing	Increases on decreasing the spacing

2.6 Summary

In this Chapter we briefly illustrated the optical fiber transmission systems, various grade optical fiber and its characteristics. Also summarize the linear and non-linear properties of the optical fiber. Then discuss about uses of optical fiber in WDM technology.

CHAPTER 3

Analytical Model

3.1 Introduction

In order to meet the huge capacity demands imposed on the core transmission network by the explosive growth in data communications the number of optical channels in WDM optical networks is being increased. Since the gain bandwidth of EDFAs is limited, these requirements for a very large number of channels mean that the channel spacing will have to be small. The current ITU grid specifies 100 GHz channel spacing, but systems are being considered with 50 GHz to 25GHz channel spacing. At these spacing, the non-linear effects of the optical fiber can induce serious system impairments. FWM is one of the major limiting factors in WDM optical fiber communication systems that use low dispersion fiber or narrow channel spacing. For long distance light wave communication larger information transmission capacity and longer repeater-less distance are required for high bit rate and WDM system for increasing bit rate. When high power optical signal is launched into a fiber linearity of optical response is lost. FWM is due to changes in the refractive index with optical power called optical Kerr effect. In FWM, three co-propagating waves produce a new optical sideband waves at different frequencies. When new frequencies fall in the transmission window of original frequency it causes severe cross talk between channels propagating through an optical fiber which limits the bandwidth of system and degrades the overall system performance. Therefore, in order to realize very long broadband optical fiber links, it is of utmost importance to compensate and suppress the pulse spreading due to FWM by a FWM suppressing model. For that reason, we need a comprehensive model for WDM transmission system with all system parameters which can predict the effect of FWM and so that suppression can be made in an effective way.

3.2 System model

The block diagram of a multi span multi-channel WDM system with EDFA in cascade used for theoretical analysis is shown in Fig. 3.1. The N channels are multiplexed by WDM MUX and the composite signal is transmitted through an optical fiber. To describe the FWM model in WDM transmission system, we assume that three channel are pump which are operated at 1559 nm with 0.8nm channel spacing. Hence, the new wave is generated at the end of propagation which can be

measured by optical spectrum analyzer. The in-line EDFA's are used in cascade to compensate the fiber losses. Finally, the composite signal is de-multiplexed at WDM DEMUX and from the modulated carrier; original signal is recovered through IM-DD method.

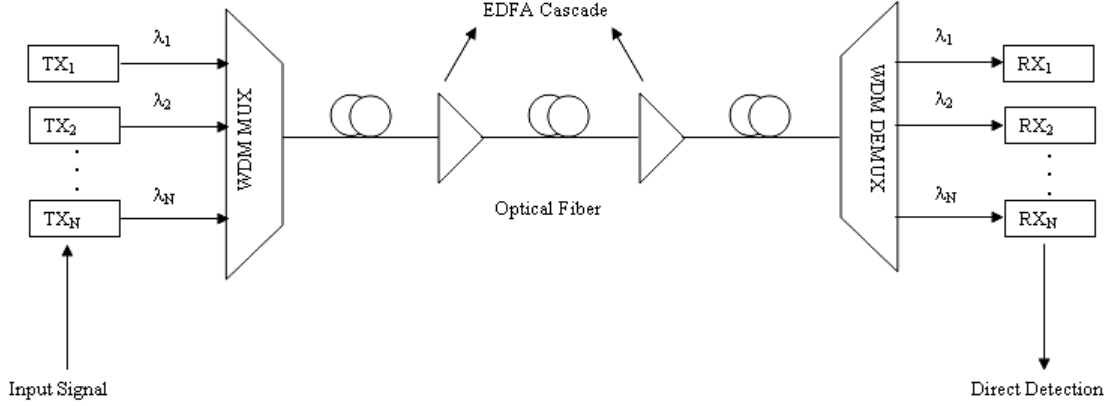


Fig. 3.1: Block diagram of a WDM system with EDFA in cascade

3.3 FWM suppression model

Considering three pump waves at frequencies ω_2, ω_3 and ω_4 are mixed and propagation constant β and generated a new wave at frequency ω_1 through the FWM process. The coupled schrödinger equations for all four waves can be written as follows:

$$\frac{d}{dz} A_1 = -\frac{1}{2} \alpha A_1 + 2i\gamma(2|A_2|^2 + 2|A_3|^2 + 2|A_4|^2)A_1 + \frac{1}{3} Gi\gamma A_2 A_3 A_4 \exp(i\Delta\beta z) \quad (3.1a)$$

$$\frac{d}{dz} A_2 = -\frac{1}{2} \alpha A_2 + i\gamma(2|A_1|^2 + 2|A_3|^2 + 2|A_4|^2)A_2 \quad (3.1b)$$

$$\frac{d}{dz} A_3 = -\frac{1}{2} \alpha A_3 + i\gamma(2|A_1|^2 + 2|A_2|^2 + 2|A_4|^2)A_3 \quad (3.1c)$$

$$\frac{d}{dz} A_4 = -\frac{1}{2} \alpha A_4 + i\gamma(2|A_1|^2 + 2|A_2|^2 + 2|A_3|^2)A_4 \quad (3.1d)$$

In the above expressions, $A_j(z)$ is the complex electric field envelopes of the wave at frequency ω_j with propagation constant β_j ($j = 1, 2, 3, 4$) and G is degeneracy factor where $G = 3$ or 6 . And γ is nonlinear parameter. Where $\gamma = 2\pi n_2 / \lambda A_{eff}$ Also, the phase-matching factor.

$$\Delta\beta = \beta(f_i) + \beta(f_j) - \beta(f_k) - \beta(f_F) \quad (3.2)$$

Where, β is the propagation constant. The efficiency of the FWM light takes place for $\Delta\beta = 0$. In this situation, the phase-matching condition is satisfied. Here, we consider the phase-mismatching $\Delta\beta$ around the zero-dispersion wavelength. β can be expanded as follows,

$$\begin{aligned} \beta(f) &= \beta(f_0) + (f - f_0) \frac{d\beta}{df}(f_0) + \frac{1}{2}(f - f_0)^2 \frac{d^2\beta}{df^2}(f_0) + \frac{1}{6}(f - f_0)^3 \frac{d^3\beta}{df^3}(f_0) \\ \Delta\beta &= \beta(f) - \beta(f_0) \\ &= (f - f_0) \frac{d\beta}{df}(f_0) - \frac{1}{2}(f - f_0)^2 \frac{\lambda^2\pi}{c} D_c(f_0) + \frac{1}{6}(f - f_0)^3 \frac{\lambda^4\pi}{3c^2} \left\{ \frac{2}{\lambda} D_c(f_0) + \frac{dD_c}{d\lambda}(f_0) \right\} \end{aligned} \quad (3.3)$$

We know that $\frac{d^2\beta}{df^2}$ is first-order group velocity dispersion and $\frac{d^3\beta}{df^3}$ is second order group velocity dispersion. We can neglect $(f - f_0) \frac{d\beta}{df}(f_0)$ from equation (3.3), because it

produces a phase delay of the carrier signal and has no influence on distortion of the signal and f is light frequency and D_c is the fiber chromatic dispersion. This expression can be used in the wavelength range, within which the dispersion slope is linear, i.e., the second-order dispersion is constant. So, we can rewrite the equation (3.3) as,

$$\Delta\beta = -\frac{1}{2}(f - f_0)^2 \frac{\lambda^2\pi}{c} D_c(f_0) + \frac{1}{6}(f - f_0)^3 \frac{\lambda^4\pi}{3c^2} \left\{ \frac{2}{\lambda} D_c(f_0) + \frac{dD_c}{d\lambda}(f_0) \right\} \quad (3.4)$$

If we use the FWM relationship of the FWM light with pump lights, $f_F = f_i + f_j - f_k$ and considering only first order dispersion for simplicity then equation (3.4) becomes,

$$\Delta\beta = \frac{2\pi\lambda^2}{c} \Delta f_{ijk} D_c \quad (3.5)$$

From equation (3.1a) – (3.1d), considering the induced depletion of the pump waves has been neglected; hence the solution for the pump envelopes can be obtained as follows:

$$A_2(z) = A_2(0) \exp\left(\frac{-\alpha z}{2}\right) \exp[-i\gamma(|A_2(0)|^2 + 2|A_3(0)|^2 + 2|A_4(0)|^2)] \exp\left(\frac{-\alpha z}{\alpha}\right) \quad (3.6a)$$

$$A_3(z) = A_3(0) \exp\left(\frac{-\alpha z}{2}\right) \exp[-i\gamma(2|A_2(0)|^2 + |A_3(0)|^2 + 2|A_4(0)|^2)] \exp\left(\frac{-\alpha z}{\alpha}\right) \quad (3.6b)$$

$$A_4(z) = A_4(0) \exp\left(\frac{-\alpha z}{2}\right) \exp[-i\gamma(2|A_2(0)|^2 + 2|A_3(0)|^2 + |A_4(0)|^2)] \exp\left(\frac{-\alpha z}{\alpha}\right) \quad (3.6c)$$

Substituting equation (3.6a) – (3.6c) into equation (3.1a), we obtain:

$$\begin{aligned} \frac{d}{dz} A_1 = & \\ & -\frac{1}{2}\alpha A_1 + 2i\gamma(|A_2(0)|^2 + |A_3(0)|^2 + |A_4(0)|^2)A_1 \exp(-\alpha z) + \\ & \frac{1}{3}Gi\gamma A_2(0)A_3(0)A_4(0) \exp\left(-\frac{3}{2}\alpha z\right) \times \exp[-i\gamma(|A_2(0)|^2 + |A_3(0)|^2 + 3|A_4(0)|^2)] \times \\ & \exp\left(\frac{-\alpha z}{\alpha}\right) \exp(i\Delta\beta z) \end{aligned} \quad (3.7)$$

Using transformation

$$A_1(z) = B_1(z) \exp\left(-\frac{\alpha z}{2}\right) \quad (3.8)$$

We can write equation (3.7) as

$$\begin{aligned} \frac{d}{dz} B_1 = & \\ & 2i\gamma(P_2 + P_3 + P_4)B_1 \exp(-\alpha z) + \frac{1}{3}Gi\gamma(P_2P_3P_4)^{1/2} \exp(i\phi_0) \exp(-\alpha z) \times \exp[-i\gamma(P_2 + P_3 + \\ & 3P_4)] \times \exp\left(\frac{-\alpha z}{\alpha}\right) \exp(i\Delta\beta z) \end{aligned} \quad (3.9)$$

Here, $\phi_0 = \phi_2(0) + \phi_3(0) - \phi_4(0)$, where ϕ_j ($j = 2,3,4$) are the initial phases for the three pump waves, respectively. Also, $P_j = |A_j(0)|^2$ ($j = 2,3,4$) are the input powers for three waves, respectively.

To represent the fiber attenuation effect on the pump waves, we use the following transformation:

$$B_1(z) = C_1(z) \exp\left[-\frac{im_1}{\alpha} \exp(-\alpha z)\right] \quad (3.10)$$

Where, $m_1 = 2\gamma(P_2 + P_3 + P_4)$. Substituting equation (3.10) into equation (3.9), we obtain the following equation for $C_1(z)$:

$$\frac{d}{dz} C_1 = \frac{1}{3}Gi\gamma(P_2P_3P_4)^{1/2} \exp\left[i\phi_0 - \alpha z + i\Delta\beta z + \frac{im_1}{\alpha} \exp(-\alpha z)\right] \quad (3.11)$$

Where, $m_p = \gamma(P_2 + P_3 - P_4)$ (3.12)

Integrating (3.11) over the fiber length L , we obtain

$$C_1 = \frac{1}{3}Gi\gamma(P_2P_3P_4)^{1/2} \exp(i\phi_0) \int_0^L \exp\left[-\alpha z + i\Delta\beta z + \frac{im_1}{\alpha} \exp(-\alpha z)\right] \quad (3.12)$$

An exact evaluation of (3.12) requires numerical integration. This is because of the presence of the nonlinear, intensity dependent phase term $\frac{im_1}{\alpha} \exp(-\alpha z)$, which decays exponentially along the fiber. An excellent approximation of integration can be obtained by recognizing that this nonlinear phase term has its greatest affect for small values of z , since the amplitude of the integrand decreases exponentially with increasing values of z . In the range $0 < z < L_{eff}$, the nonlinear phase term is well approximated by the linear expression

$$\frac{im_1}{\alpha} \exp(-\alpha z) \approx \frac{im_1}{\alpha} \left\{ 1 - \frac{1 - \exp(-\alpha L_{eff})}{L_{eff}} z \right\} \quad (3.13)$$

Where, the fiber effective length L_{eff} is defined by

Errors (3.13) for $L_{eff} < z < L$ will have a negligible effect on integration part, since the integrand is small in this range. Using (3.13) to evaluate (3.12) results in a closed form expression. Substituting this expression into (3.11) yields

$$C_1 = \frac{1}{3} Gi\gamma(P_2P_3P_4)^{1/2} \exp(i\phi_0) \exp\left[\frac{i\gamma}{\alpha}(P_2 + P_3 - P_4)z\right] \times \left\{ \frac{\exp(-\alpha L + i\Delta\beta' L) - 1}{i\Delta\beta' - \alpha} \right\} \quad (3.14)$$

Where, $\Delta\beta'$ is the new, intensity-dependent phase-matching factor, given by

$$\Delta\beta' = \Delta\beta - \gamma(P_2 + P_3 - P_4) \left\{ \frac{1 - \exp(-\alpha L_{eff})}{\alpha L_{eff}} \right\} \quad (3.15)$$

Where $\Delta\beta$ is the linear phase-matching factor given in equation (3.5). Substituting (3.14) into (3.10) and then substituting the resulting expressions into (3.8), we finally obtain the generated FWM power

$$\begin{aligned} P_{FWM}(L) &= |A_1|^2 \\ &= \frac{1}{9} G^2 \gamma^2 P_2 P_3 P_4 \exp(-\alpha L) \left\{ \frac{[1 - \exp(-\alpha L_{eff})]^2}{\alpha^2} \right\} \times \frac{\alpha^2}{\alpha^2 + (\Delta\beta')^2} \left\{ 1 + \frac{4 \exp(-\alpha L) \sin^2(\Delta\beta' L/2)}{[1 - \exp(-\alpha L)]^2} \right\} \\ P_{FWM} &= \frac{4\pi^2 n_2^2}{9\lambda^2 A_{eff}^2} G^2 P_2 P_3 P_4 \exp(-\alpha L) \left\{ \frac{[1 - \exp(-\alpha L_{eff})]^2}{\alpha^2} \right\} \times \frac{\alpha^2}{\alpha^2 + (\Delta\beta')^2} \left\{ 1 + \frac{4 \exp(-\alpha L) \sin^2(\Delta\beta' L/2)}{[1 - \exp(-\alpha L)]^2} \right\} \end{aligned} \quad (3.16)$$

The final expression of FWM power of the suppression model is expressed in term of input power

of P_j ($j = 2,3,4$), the core effective Area, A_{eff} . Dispersion, D_c and channel spacing can be measured by the expression of $\Delta\beta'$. So, it can be a comprehensive model for FWM suppression for WDM transmission system.

3.4 Bit error rate (BER)

Optical receivers convert incident optical power into electric current through a photodiode. Among a group of optical receivers, a receiver is said to be more sensitive if it achieves the same performance with less optical power incident on it. The communications system performance is characterized by a quantity called the bit error rate (BER) which is defined as the average probability of incorrect bit identification of a bit by the decision circuit of the receiver. For example, a BER of 2×10^{-6} would correspond to on average 2 errors per million bits. A commonly used criterion for digital optical receivers requires $BER \leq 1 \times 10^{-12}$. It is important for the signal to have minimum distortions in order to avoid a high BER at the receiver. This means that although the combined effects of GVD and FWM cannot be eliminated they need to be reduced so that the pulse can propagate with minimum distortions. Also the inevitable presence of amplifier noises can also cause pulse distortions and hence cause system degradation. In order to assess the system performance one needs to know how to calculate the BER of the system at the receiver end. Here we calculate the BER of the system at the receiver in the presence of amplifier noises.

In any communication system the BER is the most important factor. A standard BER in communication system sometimes is maintained. For video, speech, data and every information the separate BER is maintained. BER is related to the Input signal power and also SNR. As the input signal power is increases the BER decreases.

$$BER = \frac{\text{Number of bits receiver with error}}{\text{Total number of bits}} \quad (3.17)$$

Fig. 3.2 shows schematically the fluctuating signal received by the decision circuit, which samples it at the decision instant t_D determined through clock recovery. The sampled value I fluctuates from bit to bit around an average value I_1 or I_0 , depending on whether the bit corresponds to 1 or 0 in the bit stream. The decision circuit compares the sampled value with the threshold value I_D and calls it bit 1 if $I > I_D$ or bit 0 if $I < I_D$.

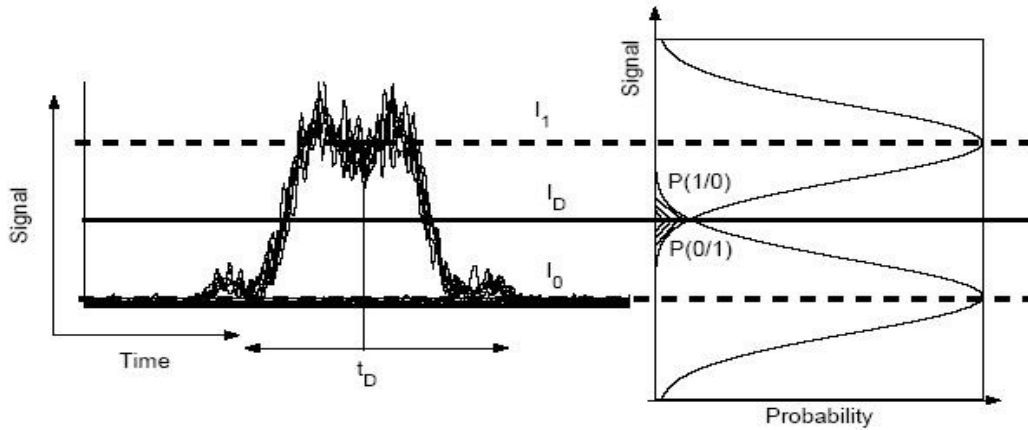


Fig. 3.2: Bit error probabilities

An error occurs if $I < I_D$ for bit 1 or if $I > I_D$ for bit 0 due to amplifier noises that add into the signal in the system. Both sources of errors can be included by defining the error probability as

$$\text{BER} = p(1)P(1/0) + p(0)P(0/1); \quad (3.18)$$

where $p(1)$ and $p(0)$ are the probabilities of receiving bits 1 and 0, respectively, $P(0/1)$ is the probability of deciding 0 when 1 is received, and $P(1/0)$ is the probability of deciding 1 when 0 is received. Since 1 and 0 bits are equally likely to occur, then we can assume, $p(1) = p(0) = 1/2$, and the BER becomes

$$\text{BER} = 1/2[P(1/0) + P(0/1)] \quad (3.19)$$

Fig. 3.2 shows how $P(0/1)$ and $P(1/0)$ depend on the probability density function $p(I)$ of the sampled value I . The functional form of $p(I)$ depends on the statistics of noise sources responsible for current fluctuations. Assuming a Gaussian noise profile, one can write the functional form of $P(0/1)$ and $P(1/0)$ as

$$P(0/1) = \frac{1}{\sqrt{2}} \int_{-\infty}^{I_D} \exp\left(-\frac{(I - I_1)^2}{2 \sigma_1^2}\right) dI \quad (3.20)$$

$$P(1/0) = \frac{1}{\sqrt{2}} \int_{I_D}^{\infty} \exp\left(-\frac{(I - I_0)^2}{2 \sigma_0^2}\right) dI \quad (3.21)$$

where σ_1^2 and σ_0^2 are the corresponding noise variances. From the definition of the complementary error function we have

$$\text{erfc}(x) = \frac{2}{\sqrt{\pi}} \int_x^{\infty} \exp(-x^2) dx \quad (3.22)$$

using eq. (3.32.) in eq.(3.30) and (3.31) we get

$$P(0/1) = \frac{1}{2} \operatorname{erfc} \left(-\frac{(I_1 - I_D)}{\sqrt{2} I_1} \right) \quad (3.23)$$

$$P(1/0) = \frac{1}{2} \operatorname{erfc} \left(-\frac{(I_D - I_0)}{\sqrt{2} I_0} \right) \quad (3.24)$$

using eqs. (3.33) and (3.34) in eq. (3.29) we can write the BER as

$$BER = \frac{1}{4} \left[\operatorname{erfc} \left(\frac{(I_1 - I_D)}{\sqrt{2} I_1} \right) + \operatorname{erfc} \left(\frac{(I_D - I_0)}{\sqrt{2} I_0} \right) \right] \quad (3.25)$$

eq (3.35) shows that the BER depends on the decision threshold I_D .

The required SNR to maintain particular bit error rates may be obtained using procedure adopted for error performance of electrical digital systems where the noise distribution is considered to be white Gaussian. This Gaussian approximation is sufficiently accurate for design purposes and is far easier to evaluate than the more exact probability distribution within the receiver.

3.5 Noises in Optical receiver

Two types of noises, such as, thermal noise and shot noise are considered and also assumed that all these noises have Gaussian distribution those occur in at the optical receiver. It is assumed that lights from all optical sources have an identical state of polarization, which corresponds to considering the worst case situation for system degradation.

3.5.1 Thermal noise

Thermal noise is the spontaneous fluctuation due to thermal interaction between, say, the free electrons and the vibrating ions in a conducting medium, and it is especially prevalent in resistors at room temperature. The thermal noise current is mean square value is given below.

$$P_{\text{th}} = \text{Thermal noise} = 4kTB/R_L \quad (3.26)$$

Where, k = Boltzmann's constant, T =Absolute temperature and B = Post detection bandwidth of the system

3.5.2 Shot noise

Shot noise occurs due to radiation. In fiber optic communication system, due to background radiation, some electron or charge penetrate rapidly and generate noise. The noise in mean square value is given below.

$$P_{\text{shot}} = \text{Shot noise} = 2eI_sB \quad (3.27)$$

Where,

e= Charge on an electron

I_s = Current

B= Post detection bandwidth of the system.

3.5.3 Expression of BER on FWM

The probability of error or bit Error rate (BER) is given by

$$BER(P_e) = 0.5\text{erfc}[SNR] \quad (3.28)$$

$$\text{where, } SNR(r) = \frac{I_s}{\sqrt{2}} \quad (3.29)$$

$$\text{where } I_s = R_d P_s(r) \quad (3.30)$$

$$\text{and } = \sqrt{P_{th} + P_{shot} + P_{FWM}} \quad (3.31)$$

$$\text{where } P_{th} = \frac{4kTB}{R_L}$$

$$\text{and, } P_{shot} = 2eI_sB$$

where B=Bandwidth, e= Electron charge

and P_{FWM} = Normalized FWM power transfer function.

$$\begin{aligned} &= \frac{1}{9} G^2 \gamma^2 P_2 P_3 P_4 \exp(-\alpha L) \left\{ \frac{[1 - \exp(-\alpha L_{eff})]^2}{\alpha^2} \right\} \\ &\quad \times \frac{\alpha^2}{\alpha^2 + (\Delta\beta')^2} \left\{ 1 + \frac{4 \exp(-\alpha L) \sin^2(\Delta\beta' L/2)}{[1 - \exp(-\alpha L)]^2} \right\} \end{aligned}$$

3.6 Simulation setup and description

Rsoft's OptSim simulation software is used to simulate the FWM suppression model to measure its performance in presence of various system parameters. OptSim gives us the environment almost the exact physical realization of a system. In order to illustrate FWM effect and study the impact of fiber parameters in WDM system, the system is simulated with block diagram shown in Fig. 3.3. In the diagram, the transmitter section (for the first channel) consists of data source (b301), electrical driver (b297), laser source (b300) and amplitudemodulator (b298). The electrical driver is important component that generates the desired data transmission format. It converts the logical input signal, a binary sequence of zeros and

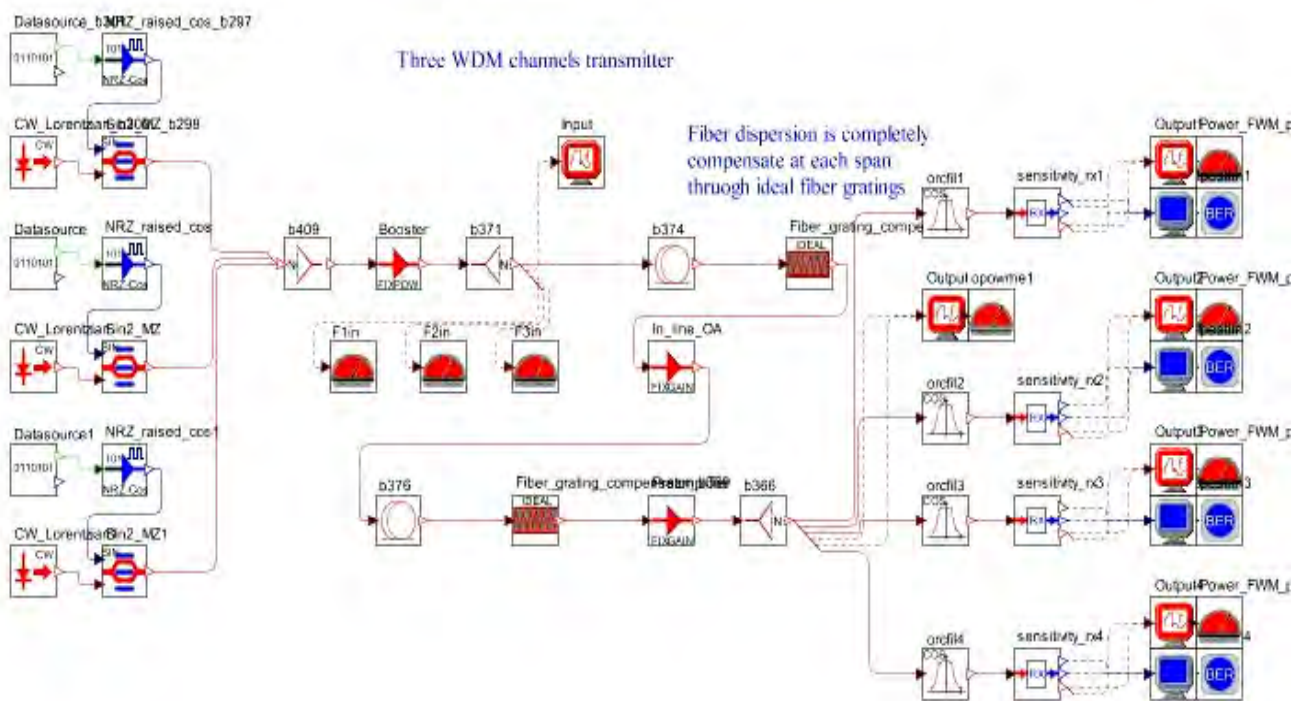


Fig. 3.3: Simulation of 3-channel WDM system

ones into an electrical signal. The output of modulator from three channels is fed to mixer (b409) where it goes to optical link through EDFA amplifier (b295). At the input, through optical splitter, three power meters (F1 in, F2 in and F3 in) tuned at different frequencies are used to measure optical signals at the input. Also, spectrum analyzer is connected for measuring input spectrum. Three WDM channels are launched over two DS fiber spans of 100 km each. Dispersion is completely compensated at each span. The receiver consists of optical filter and optical splitter (b366). One end of splitter is used to measure optical parameters and other can be fed to detector. The output of the detector can be passed through electrical filter and then to electrical splitter. The electrical filter is

connected to measuring equipment like electroscopes, and electric power meters. In this simulation only the optical parameters are measured. Four power meters (F1 op, F2 op, F3 op and F4 op) tuned at different frequencies are used to measure different optical signals at the output. The spectrum analyzer is used to measure optical spectrum at both input and output. The laser is CW Lorentzian. The amplitude modulator is of type \sin^2 with excess loss of 3 dB. The simulated bit rate is 10 GHz. The electrical filter is of the type Bessel with 0.3 dB bandwidth equal to 8 GHz. The optical splitter is ideal and optical filter is of type .Multiple Stage Lorentzian. with band pass filter synthesis with 3 stages. The detector is APD with quantum efficiency of 0.7 before avalanche gain.

3.7 Summery

In this chapter analytical derivation of FWM suppression model and also find the BER equation of the model for justification of the model with others models published. Henceforth, also describe the simulation setup of the model to find the comparative analysis of the model with the analytical model results.

CHAPTER 4

Result and Discussion

4.1 Introduction

To verify the derived theoretical expressions developed in the earlier chapter, numerical solutions have been achieved by means of MATLAB to produce graphical results by varying different parameters. Here we have used 3- types of fiber, such as- SSMF, DSF and LEAF, and compared their FWM induced crosstalk performance. Though the analytical model is developed for three-channel system We have also carried out simulation to find the impact of FWM for DSF fiber only using OptSim simulation software. Different system parameters of 3- types of fiber are shown in Table 4.1.

Table 4.1: Different system parameters

Parameter (unit)	SSMF	DSF	LEAF
Probe wavelength (nm)	1559	1559	1559
Channel spacing (nm)	0.4, 0.8, 1.6	0.4, 0.8, 1.6	0.4, 0.8, 1.6
Zero dispersion slope (ps/nm ² /nm)	0.095	0.075	0.084
Effective Area (m ²)	8.0X10 ⁻¹¹	5.5X10 ⁻¹¹	7.2X10 ⁻¹¹
Attenuation parameter (dB/km)	0.25	0.25	0.25
Dispersion Parameter (ps/nm/km)	17	3.5	4.5
First order GVD (ps ² /nm)	0.206	0.4515	0.3349
Second order GVD(ps ³ /nm)	0.192295	0.1995	0.1957
Span Length (km)	100	100	100
Input pump power (dBm)	11.5	11.5	11.5
Input Probe Power (dBm)	11.5	11.5	11.5

4.2 Crosstalk effect in SSMF

Using the developed analytical model, amount of normalized cross talk is calculated using SSMF for different parameter like channel spacing, fiber length and effective core area. We have observed the variation of FWM crosstalk in SSMF. Fig. 4.1 shows the effect of crosstalk due to different channel input power with various effective core area and Fig. 4.2 presents crosstalk vs. fiber length and Fig.

4.3 shows crosstalk vs. channel separation with various effective core area. It is found that the spectral characteristics of the fiber depend on the channel spacing, Fiber length and core effective area of the fiber. For example, at 0.8 nm and 1.6 nm channel spacing the crosstalk is -33 dB and -45 dB respectively at Fig 4.3. It is also observed that at very narrow channel spacing (≤ 0.2 GHz) the crosstalk is very negligible. At Fig. 4.5, it shows that FWM effect is decreased with increase of effective core area of the fiber.

It is observed that there is significant changes in FWM crosstalk due to different effective area while channel input power and length are increased. In Fig. 4.1 and Fig. 4.2 shows that FWM crosstalk increases when input power of the channel and length of the fiber increases. But it is noticeable in Fig. 4.3 and Fig. 4.5 that if channel separation and effective core area of the fiber increase then FWM crosstalk falls significantly. For example, the FWM crosstalk decreases from -33dB to -45dB when channel separation increase from 0.2 nm to 1.6 nm. Also in Fig. 4.4 shows the calculation of FWM crosstalk as a function of dispersion.

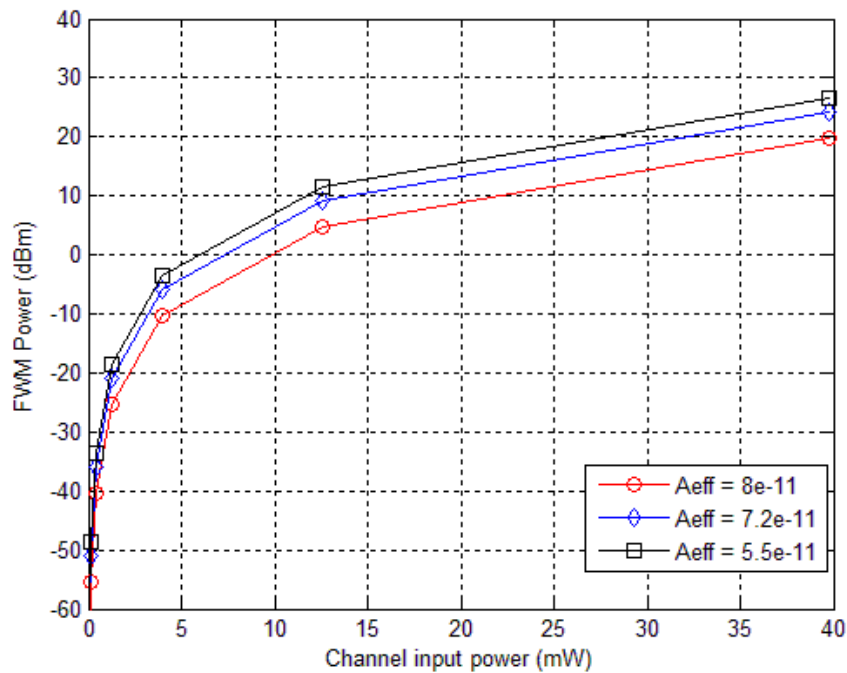


Fig. 4.1: FWM crosstalk as a function of channel input power. Where $D_c = 17\text{ps/km-nm}^2$, $\alpha = 0.25\text{dBm/km}$, $n_2 = 2.65 \times 10^{-20} \text{ m}^2/\text{w}$, $\Delta\lambda = 0.8 \text{ nm}$

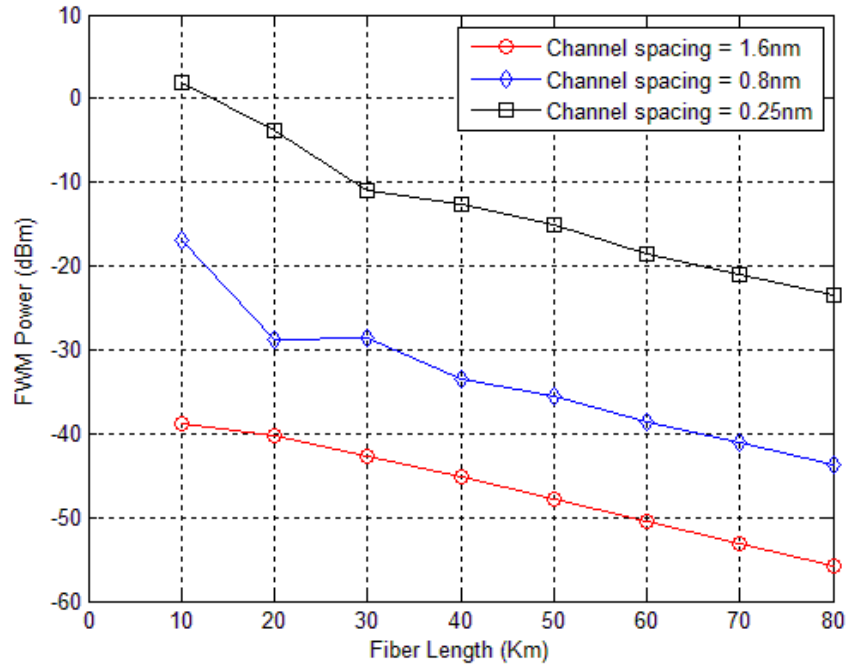


Fig. 4.2: FWM crosstalk as a function of fiber length. Where $D_c = 17\text{ps/km-nm}^2$, $\alpha = 0.25\text{dBm/km}$, $n_2 = 2.65 \times 10^{-20} \text{ m}^2/\text{w}$, $\Delta\lambda = 1.6\text{nm}$, $A_{eff} = 8.8 \mu\text{m}^2$.

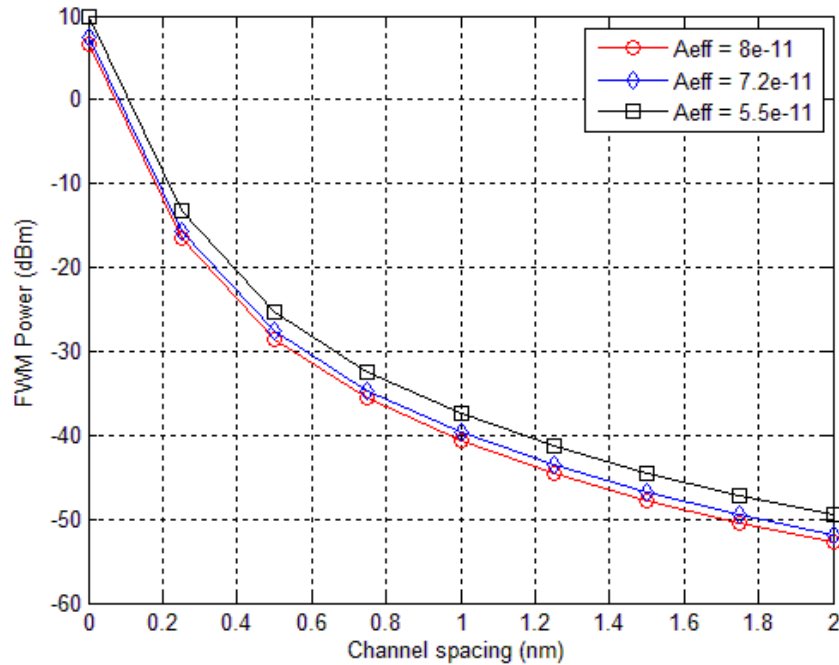


Fig. 4.3: FWM crosstalk as a function of channel spacing. Where $D_c = 17\text{ps/km-nm}^2$, $\alpha = 0.25\text{dBm/km}$, $n_2 = 2.65 \times 10^{-20} \text{ m}^2/\text{w}$, $L = 100\text{km}$.

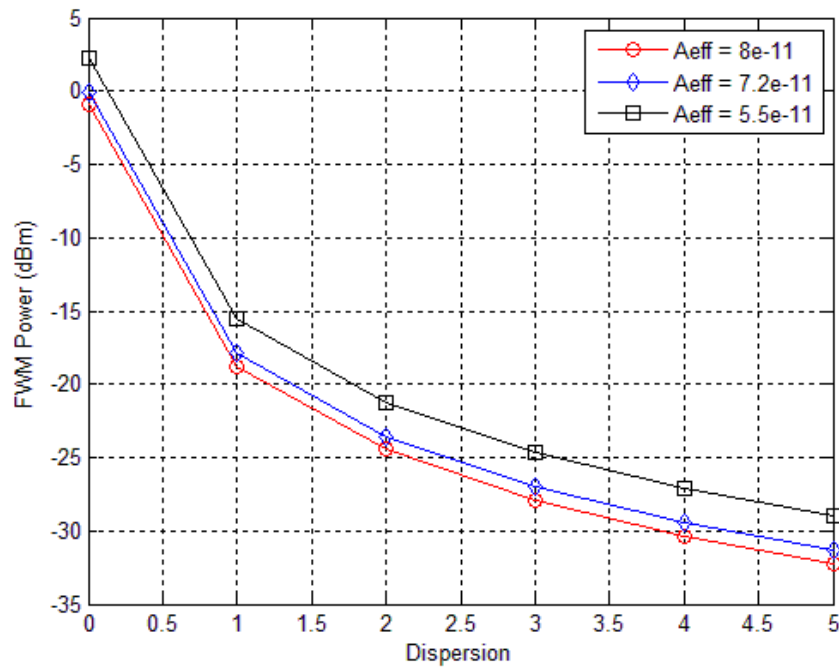


Fig. 4.4: FWM crosstalk as a function of dispersion. Where $L = 100\text{km}$, $\alpha = 0.25\text{dBm/km}$, $n_2 = 2.65 \times 10^{-20} \text{ m}^2/\text{w}$, $\Delta\lambda = 0.8 \text{ nm}$

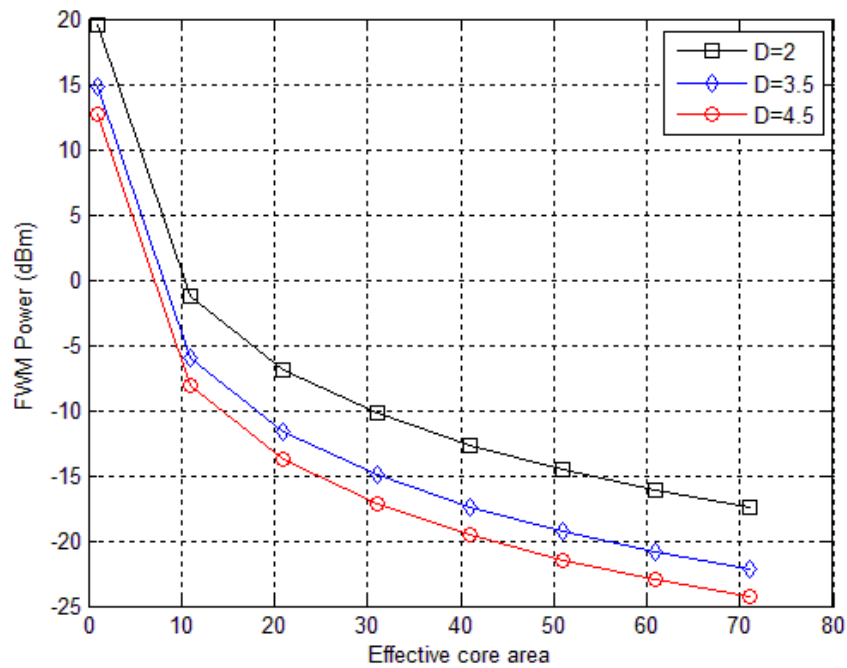


Fig. 4.5: FWM crosstalk as a function of Effective core area. Where $L = 100\text{km}$, $\alpha = 0.25\text{dBm/km}$, $n_2 = 2.65 \times 10^{-20} \text{ m}^2/\text{w}$, $\Delta\lambda = 0.8 \text{ nm}$

4.3 Crosstalk effect in DSF

Fig. 4.6 and Fig. 4.8 are plots of crosstalk in DSF fiber in variation to channel input power and wavelength separation with various effective areas. And Fig. 4.7 plots of FWM crosstalk versus fiber span length. And Fig. 4.10 plots of FWM power against effective core area of the fiber. All of these plots are similar to SSMF, but amount of crosstalk is different.

For instance (from Fig. 4.6), at 10mW channel input power, the crosstalk of FWM increases about to 25 dB. In this case, SSMF has lost more crosstalk than DSF. In Fig. 4.8 and Fig. 4.10 depicts the same results which is SSMF fiber loses more FWM power than DSF for higher effective areas and channel separations. And FWM decreases with the increase of core effective area but very small area has no FWM effect but it limits the bit rate of the fiber.

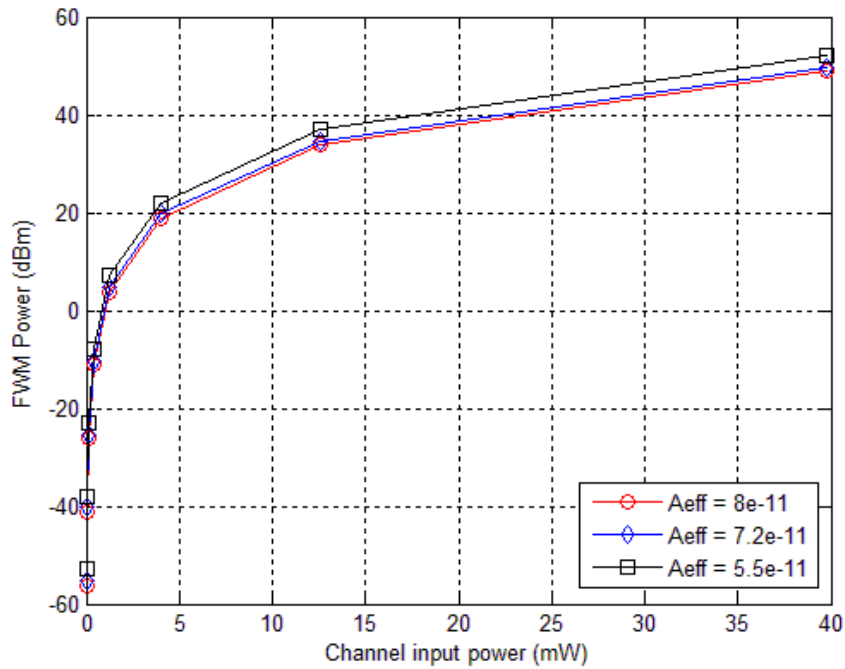


Fig. 4.6: FWM crosstalk as a function of channel input power. Where $D_c = 3.5 \text{ ps/km-nm}^2$,
 $\alpha = 0.25 \text{ dBm/km}$, $n_2 = 2.65 \times 10^{-20} \text{ m}^2/\text{w}$, $\Delta\lambda = 0.8 \text{ nm}$

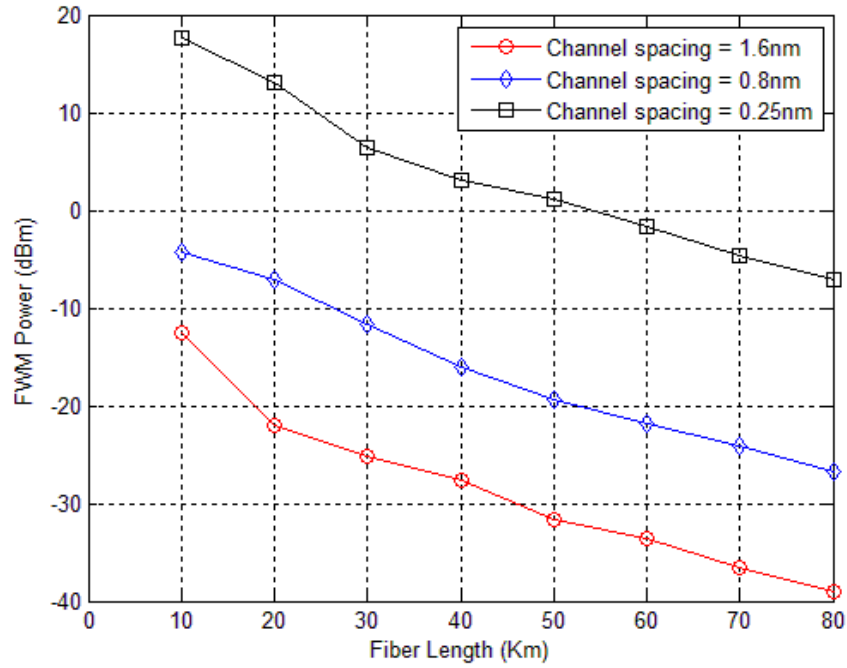


Fig. 4.7: FWM crosstalk as a function of fiber length. Where $D_c = 3.5\text{ps/km-nm}^2$, $\alpha = 0.25\text{dBm/km}$, $n_2 = 2.65 \times 10^{-20} \text{ m}^2/\text{w}$, $\Delta\lambda = 0.8 \text{ nm}$, $A_{eff} = 5.5 \mu\text{m}^2$.

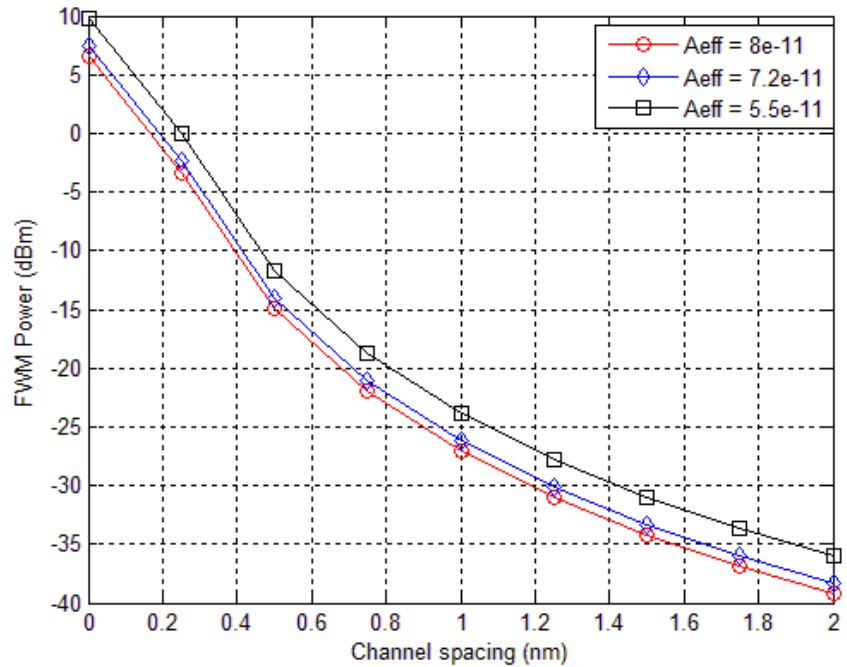


Fig. 4.8: FWM crosstalk as a function of channel spacing. Where $D_c = 3.5\text{ps/km-nm}^2$, $\alpha = 0.25\text{dBm/km}$, $n_2 = 2.65 \times 10^{-20} \text{ m}^2/\text{w}$, $L = 100\text{km}$.

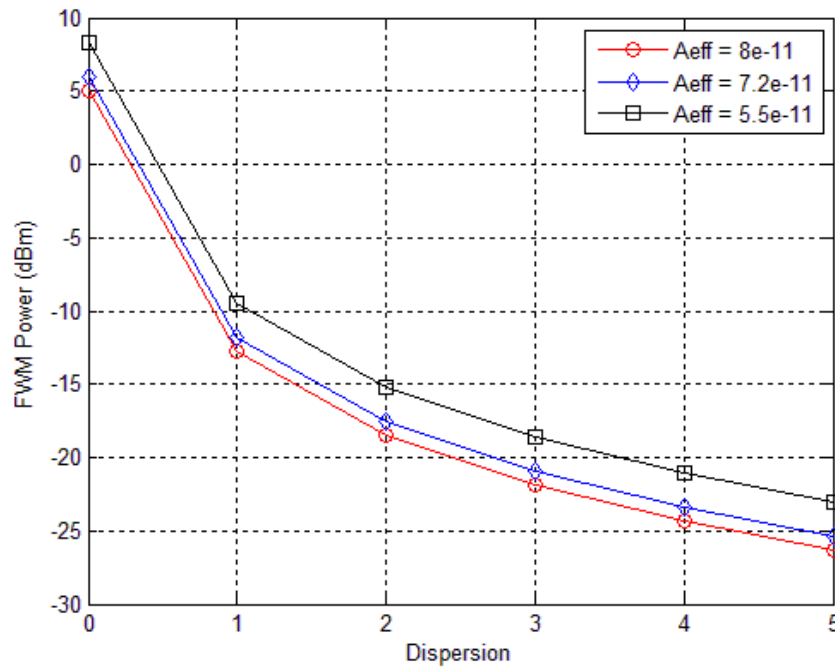


Fig. 4.9: FWM crosstalk as a function of dispersion. Where $L = 100\text{km}$,
 $\alpha = 0.25\text{dBm/km}$, $n_2 = 2.65 \times 10^{-20} \text{ m}^2/\text{w}$, $\Delta\lambda = 0.8 \text{ nm}$

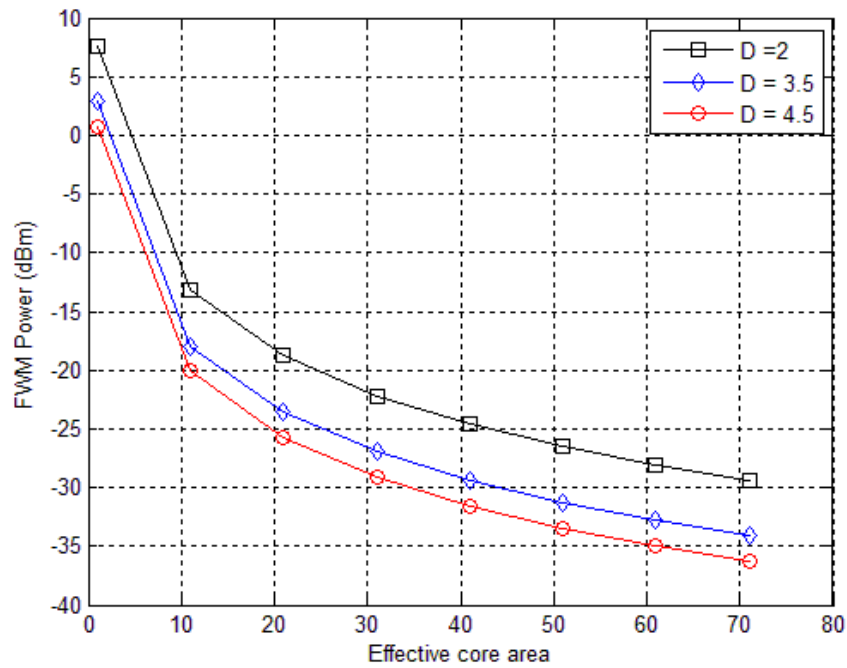


Fig. 4.10: FWM crosstalk as a function of effective core area. Where $L = 100\text{km}$,
 $\alpha = 0.25\text{dBm/km}$, $n_2 = 2.65 \times 10^{-20} \text{ m}^2/\text{w}$, $\Delta\lambda = 0.8 \text{ nm}$

4.4 Crosstalk presence in LEAF

LEAF fiber is developed by Corning Corporation Inc., USA to carry more optical power but with lower power density, alone inside core of the fiber. It operates in the wavelength 1550 nm -1575 nm ranges. LEAF fiber gives same results as found in SSMF for compensating the crosstalk of FWM but better than DSF fiber. For instance, Fig. 4.11 plots of FWM crosstalk versus input power depicts that at 12mW channel input power its shows lower FWM crosstalk 5 dB where DSF shows it above 20dB is much higher than expectation. In Fig. 4.12 and 4.13 shows the plots of FWM crosstalk with various fiber length and channel spacing for various effective areas. In Fig. 4.13 plots FWM crosstalk with channel spacing for various effective areas. The plots depicts FWM crosstalk is -25dB for channel spacing at 0.8 nm and 80 μm^2 effective area which has the significance that more channel spacing and effective area compensate more FWM crosstalk. In Fig. 4.14 shows that with the increase of dispersion parameter values it decreases the FWM effect on fiber. LEAF has its large effective area, so it depicts more suppression if we increase effective area more as shown in Fig. 4.15.

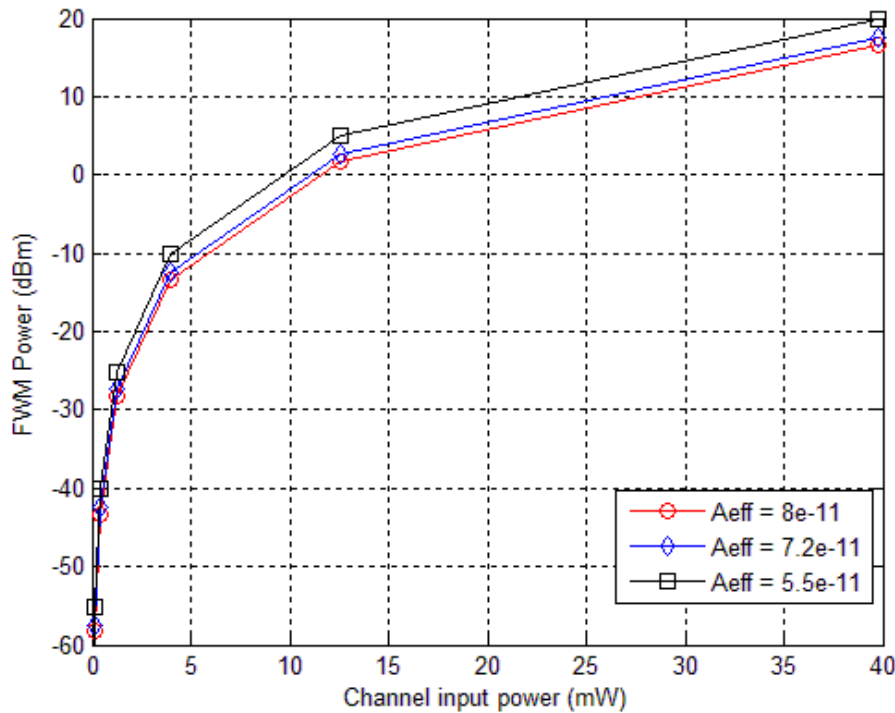


Fig. 4.11: FWM crosstalk as a function of channel input power. Where $D_c = 4.5 \text{ ps/km-nm}^2$,

$$\alpha = 0.25 \text{ dBm/km}, n_2 = 2.65 \times 10^{-20} \text{ m}^2/\text{w}, \Delta\lambda = 0.8 \text{ nm}$$

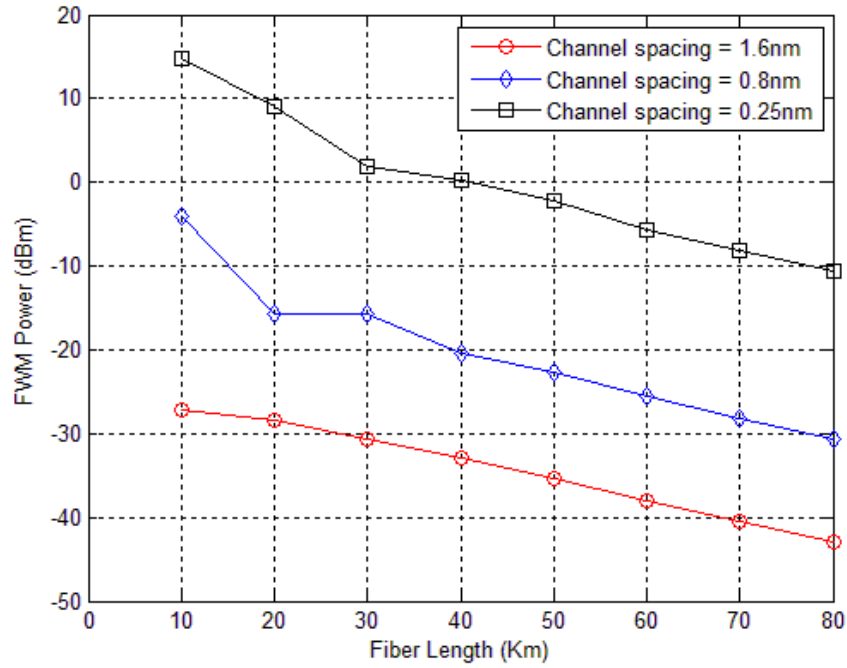


Fig. 4.12: FWM crosstalk as a function of fiber length. Where $D_c = 4.5\text{ps/km-nm}^2$, $\alpha = 0.25\text{dBm/km}$, $n_2 = 2.65 \times 10^{-20} \text{ m}^2/\text{w}$, $\Delta\lambda = 0.8 \text{ nm}$, $A_{eff} = 7.2 \mu\text{m}^2$.

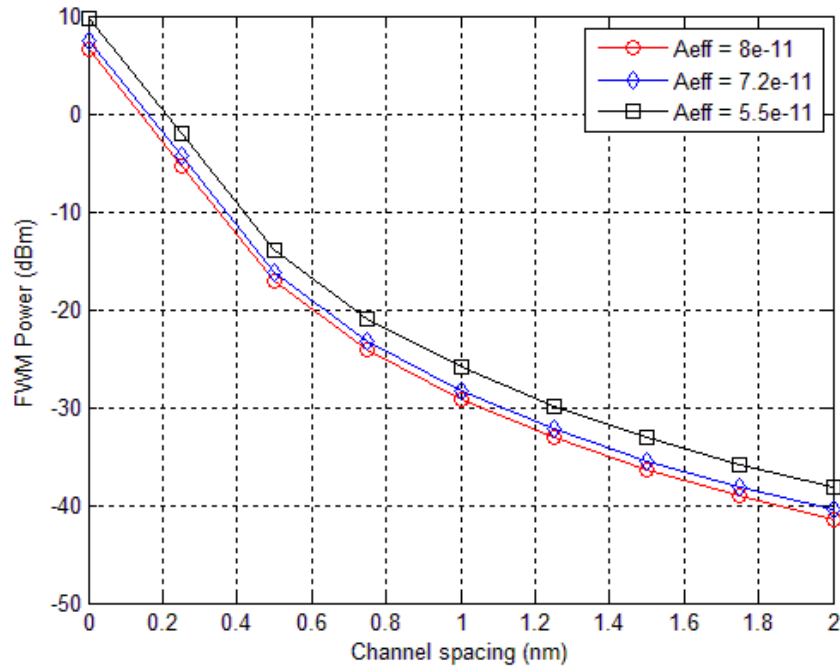


Fig. 4.13: FWM crosstalk as a function of channel spacing. Where $D_c = 4.5\text{ps/km-nm}^2$, $\alpha = 0.25\text{dBm/km}$, $n_2 = 2.65 \times 10^{-20} \text{ m}^2/\text{w}$, $L = 100\text{km}$.

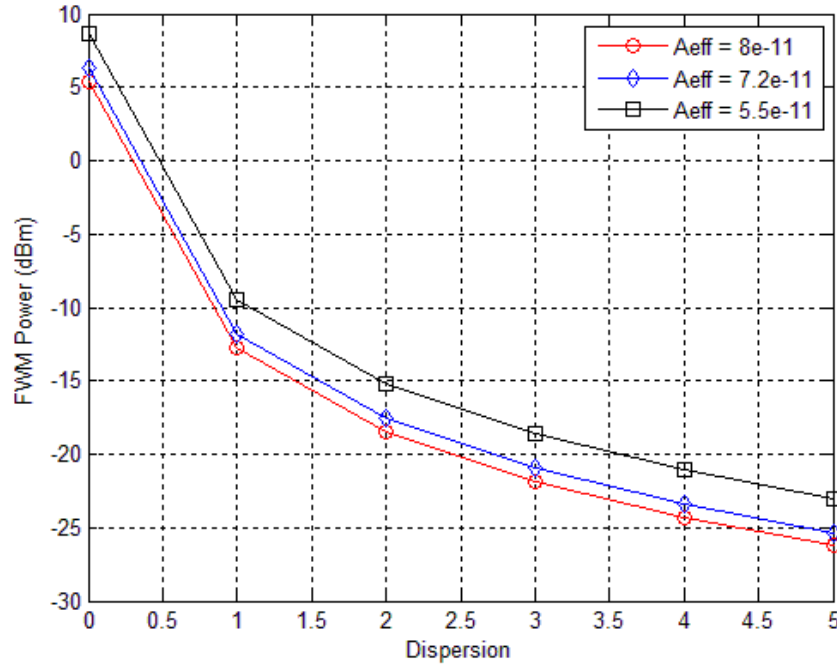


Fig. 4.14: FWM crosstalk as a function of dispersion. Where $L = 100\text{km}$,
 $\alpha = 0.25\text{dBm/km}$, $n_2 = 2.65 \times 10^{-20} \text{ m}^2/\text{w}$, $\Delta\lambda = 0.8 \text{ nm}$

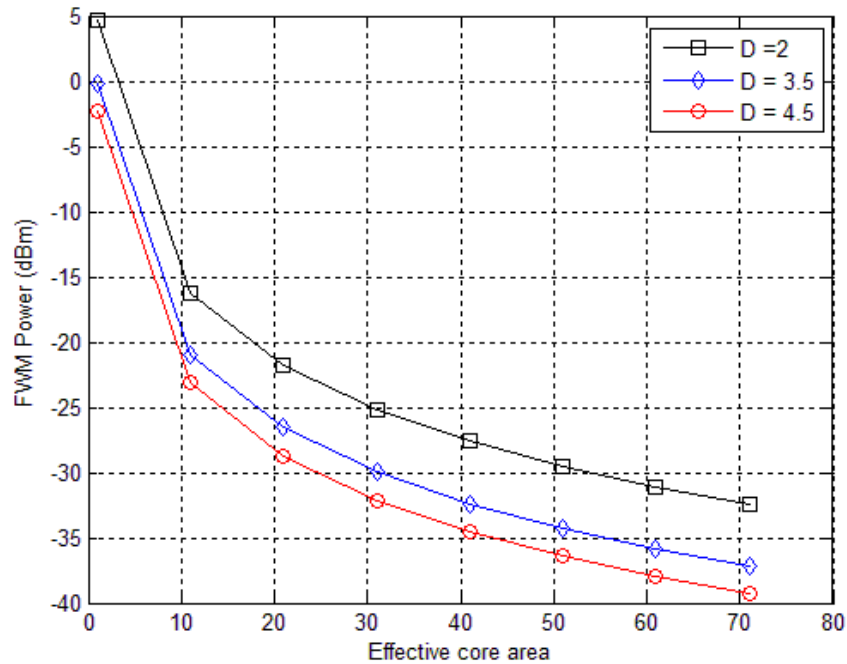


Fig. 4.15: FWM crosstalk as a function of effective core area. Where $L = 100\text{km}$,
 $\alpha = 0.25\text{dBm/km}$, $n_2 = 2.65 \times 10^{-20} \text{ m}^2/\text{w}$, $\Delta\lambda = 0.8\text{nm}$

4.5 FWM effect on all kind of optical fiber:

The plots of FWM crosstalk are plotted for various dispersion parameters; channel Spacing, effective area and channel input powers for 3-types of fiber in Fig. 4.16, Fig. 4.17, Fig. 4.18 and Fig. 4.19. It shows that FWM crosstalk decreases for higher channel spacing and dispersion parameter. In Fig. 4.16 shows that FWM crosstalk differs in each fiber is -5dB around. In Fig. 4.17 shows a significant figure that DSF and LEAF has almost same trend of plots of FWM crosstalk for any instance but SSMF has significant decreases of power. For instance, -80dB crosstalk found in Fig. 4.17 for SSMF fiber where DSF and LEAF has about -25dB and -29dB respectively. In context of input channel power, SSMF is better than other two fibers. In Fig. 4.19, for general input power for fiber at 10mW, FWM crosstalk for SSMF increases to about 5dB which is 5 ~ 7 dB lower that DSF and LEAF fiber. Considering all combined plots, it is generally concluded that SSMF fiber is more compensating fiber of FWM crosstalk.

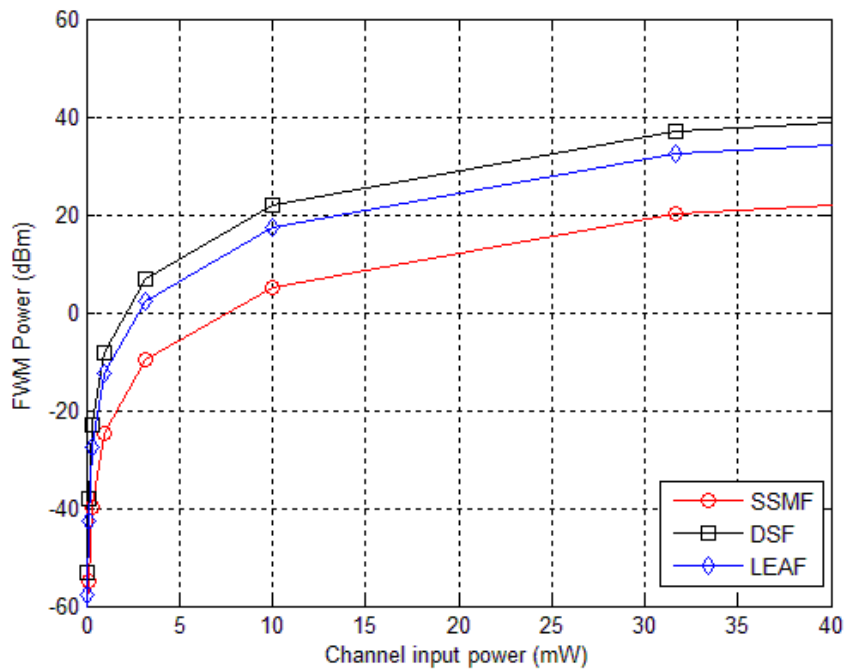


Fig. 4.16: FWM crosstalk as a function of channel input power. Where $L = 100\text{km}$,

$$\alpha = 0.25\text{dBm/km}, n_2 = 2.65 \times 10^{-20} \text{ m}^2/\text{w}, \Delta\lambda = 0.8 \text{ nm}$$

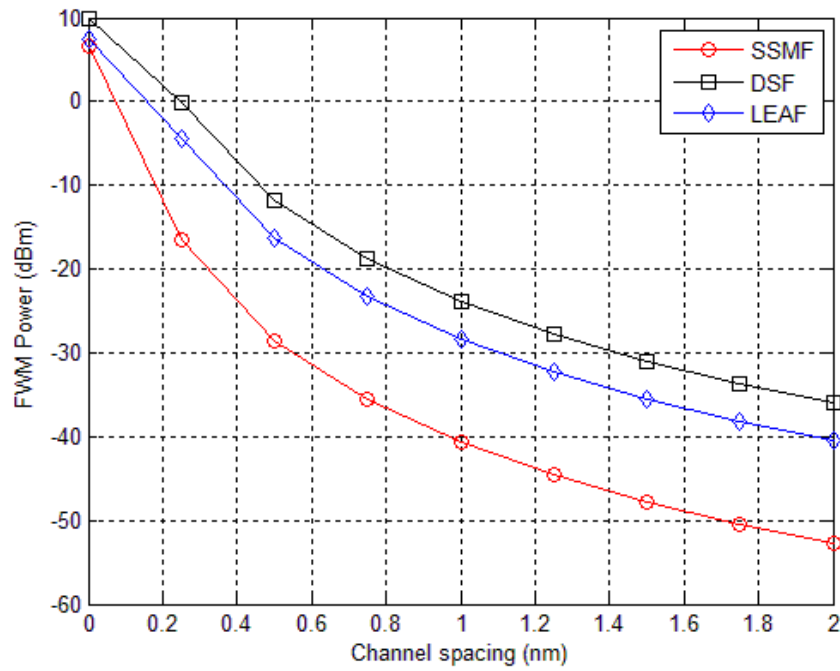


Fig. 4.17: FWM crosstalk as a function of channel spacing. Where $L = 100\text{km}$,
 $\alpha = 0.25\text{dBm/km}$, $n_2 = 2.65 \times 10^{-20} \text{ m}^2/\text{w}$, $\Delta\lambda = 0.8 \text{ nm}$

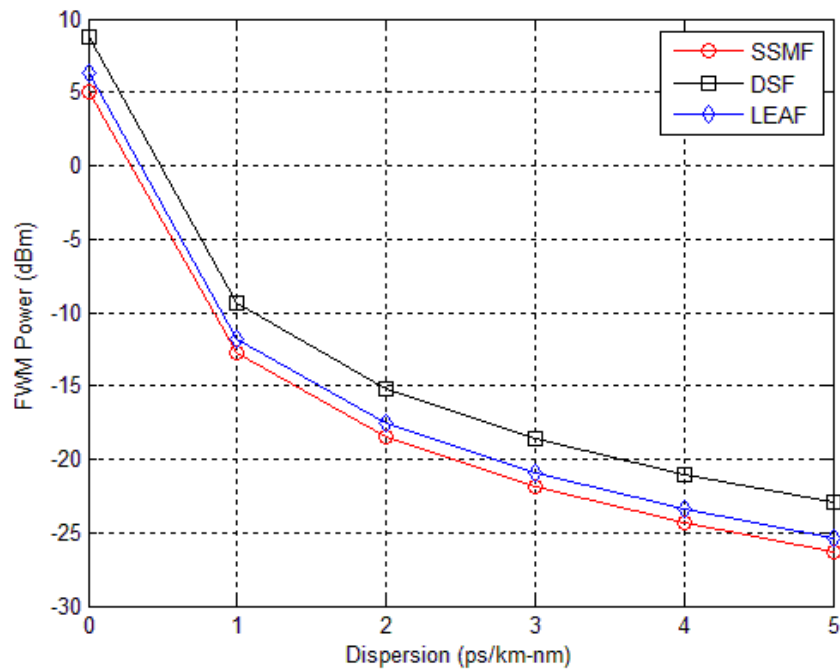


Fig. 4.18: FWM crosstalk as a function of dispersion. Where $L = 100\text{km}$,
 $\alpha = 0.25\text{dBm/km}$, $n_2 = 2.65 \times 10^{-20} \text{ m}^2/\text{w}$, $\Delta\lambda = 0.8 \text{ nm}$

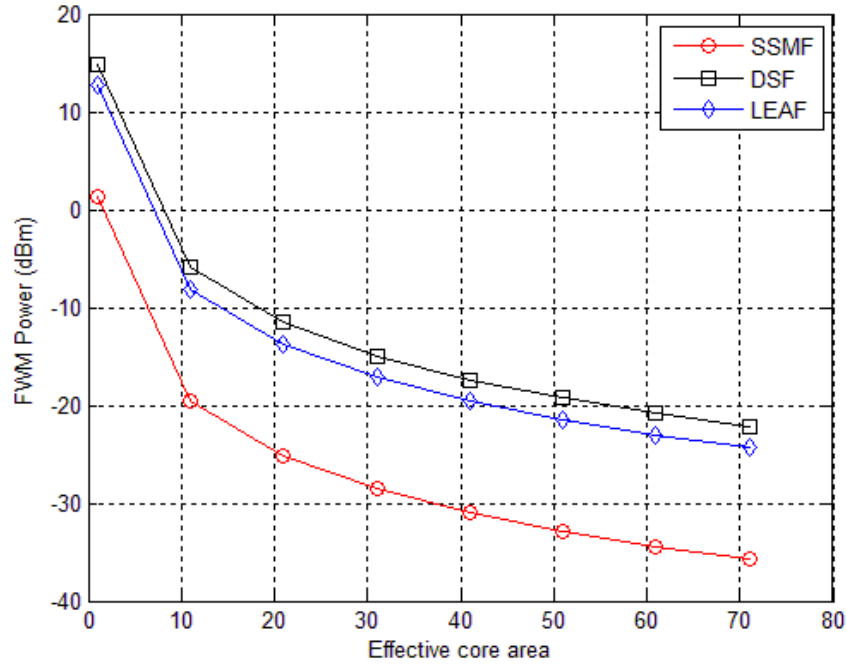


Fig. 4.19: FWM crosstalk as a function of effective core area. Where $L = 100\text{km}$,

$$\alpha = 0.25\text{dBm/km}, n_2 = 2.65 \times 10^{-20} \text{ m}^2/\text{w}, \Delta\lambda = 0.8\text{nm}$$

4.5 FWM effect on Bit Error rate (BER):

The Fig. 4.20 calculate the BER of FWM effect. For these calculation fiber loss is 0.25 dBm/km, the fiber core effective area is $55 \mu\text{m}^2$, the fiber non-linear refractive index is $n_2 = 2.65 \times 10^{-20}$, the fiber dispersion is $D_c = 17\text{ps/km-nm}^2$ at 1559 nm and dispersion-slope is 0.095 ps/km-nm^2 . The Fig. 4.20 shows that BER is improved at higher dispersion parameters value. At dispersion 4 ps/km-nm-nm it quite impressive to reach at desired BER which is 10^{-12} in WDM communication system which necessary for higher bit rate on long haul communication.

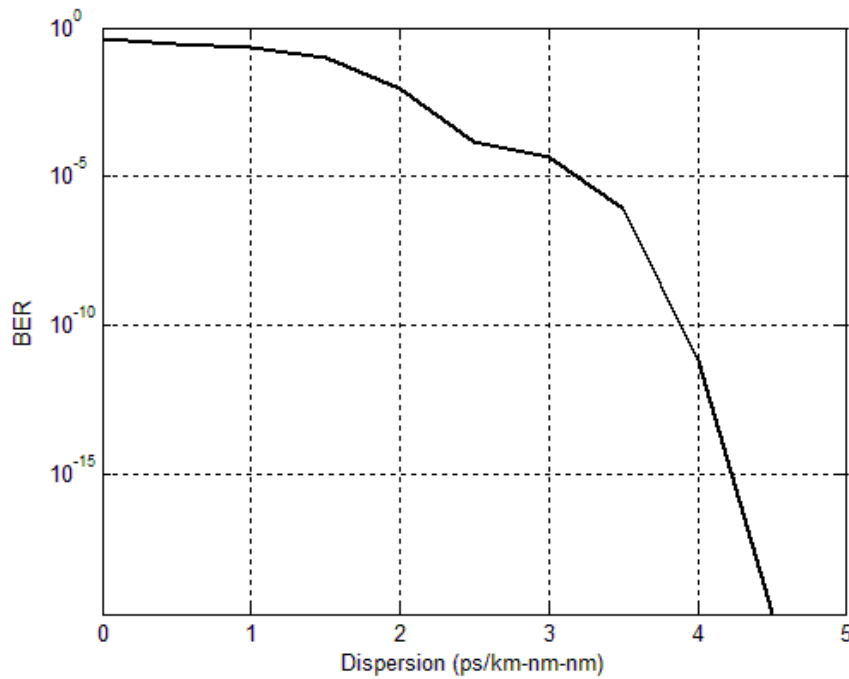


Fig. 4.20: FWM effect on Bit Error rate (BER) in dB. Where $L = 100\text{km}$, $\alpha = 0.25\text{dBm/km}$, $n_2 = 2.65 \times 10^{-20} \text{ m}^2/\text{w}$, noise bandwidth, $B = 0.35e^{-9}$, receiver sensitivity, $R_d = 0.8$.

4.6 Simulation Results

In this thesis, we also investigate the effect of FWM on WDM optical transmission system for dispersion and effective area with equal spaced channel and also plot using Rsoft's OptSim simulation software for DSF. The channels are modulated at 10 Gbps data rate with equal spaced channel by 0.8 nm, the distance between the inline optical EDFA fiber amplifiers is 100 km (span length).

4.7 Input/output spectrum

The input and output optical spectrum of the pump and probe is shown in Fig. 4.21 and Fig. 4.22 respectively. It is noticed that after propagating 100 km fiber link the optical due to the effect of fiber nonlinearity the output spectrum of three input channel are distorted and nine new frequencies are generated.

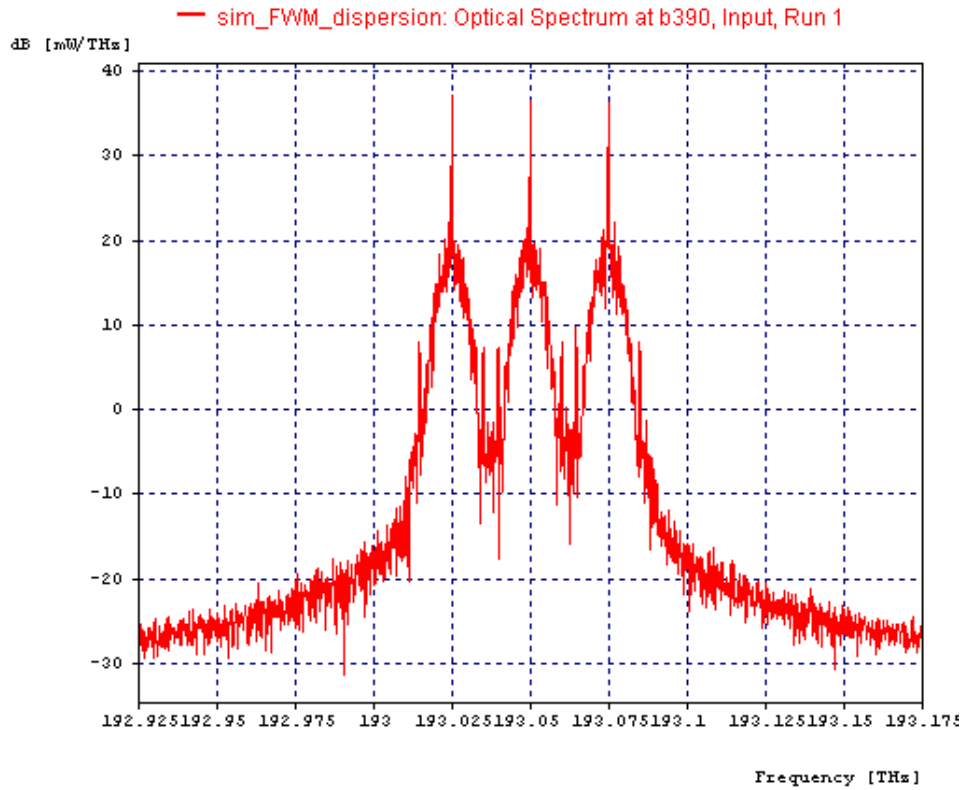


Fig. 4.21: Pump and probe optical spectrum at the input for 3-channel WDM system

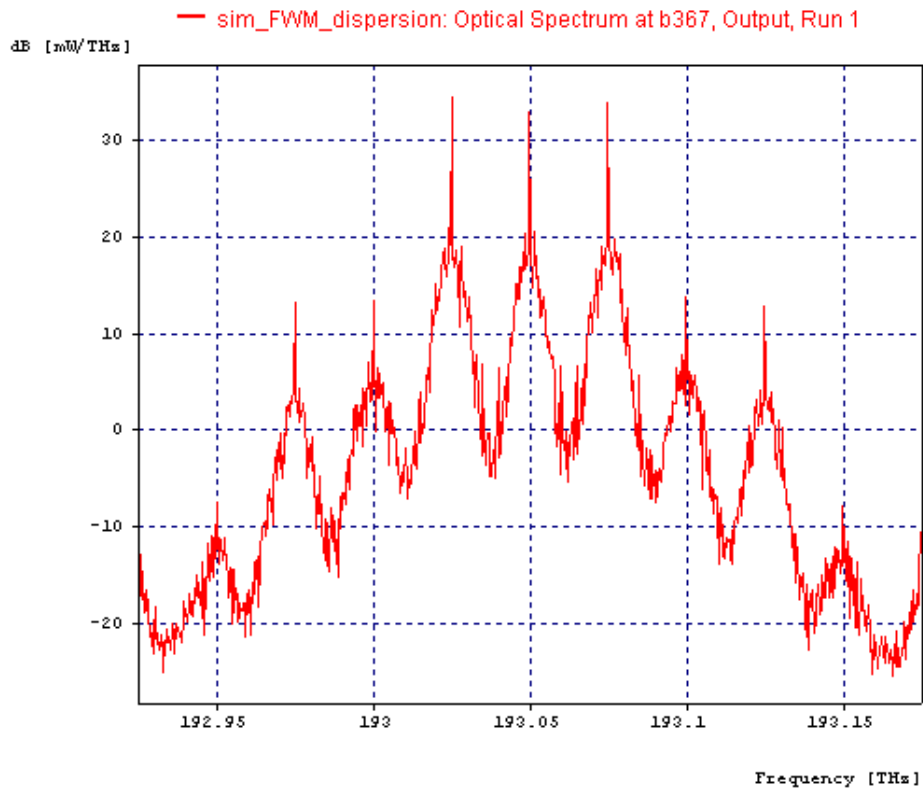


Fig. 4.22: Pump and probe optical spectrum at the output for 3-channel WDM system

4.8 FWM effect on WDM transmission system:

To assess the impact of FWM on the transmission system in electrical domain, we first implement a 3-channel WDM system and monitor the probe signal for equal spaced channel for various dispersion and effective area. We found that in Fig. 4.23 the FWM power achieved at -21dBm for dispersion at 5 ps/km-nm-nm and -44 dBm at high core effective area at $55 \mu\text{m}^2$ in DSF fiber only. We have got the same trend of plots for our comprehensive model in Fig. 4.6 to Fig. 4.10. Considering BER, in the Fig. 4.27 of simulation and Fig. 4.20 of comprehensive model got same BER at 4 ps/km-nm-nm of dispersion.

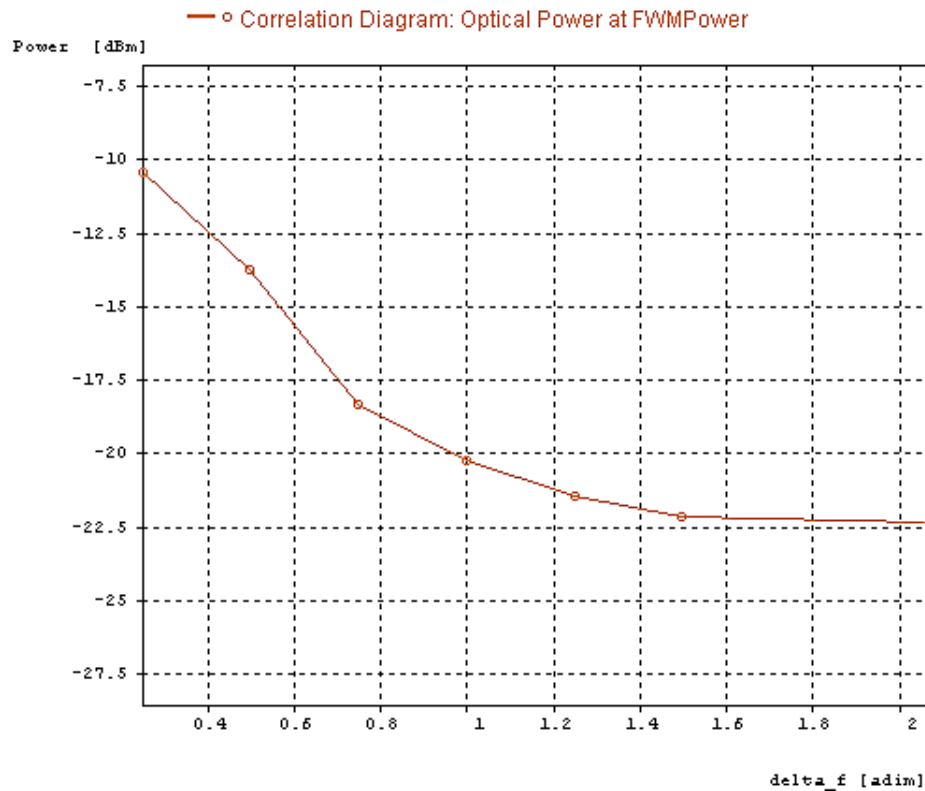


Fig. 4.23: FWM power Vs channel spacing

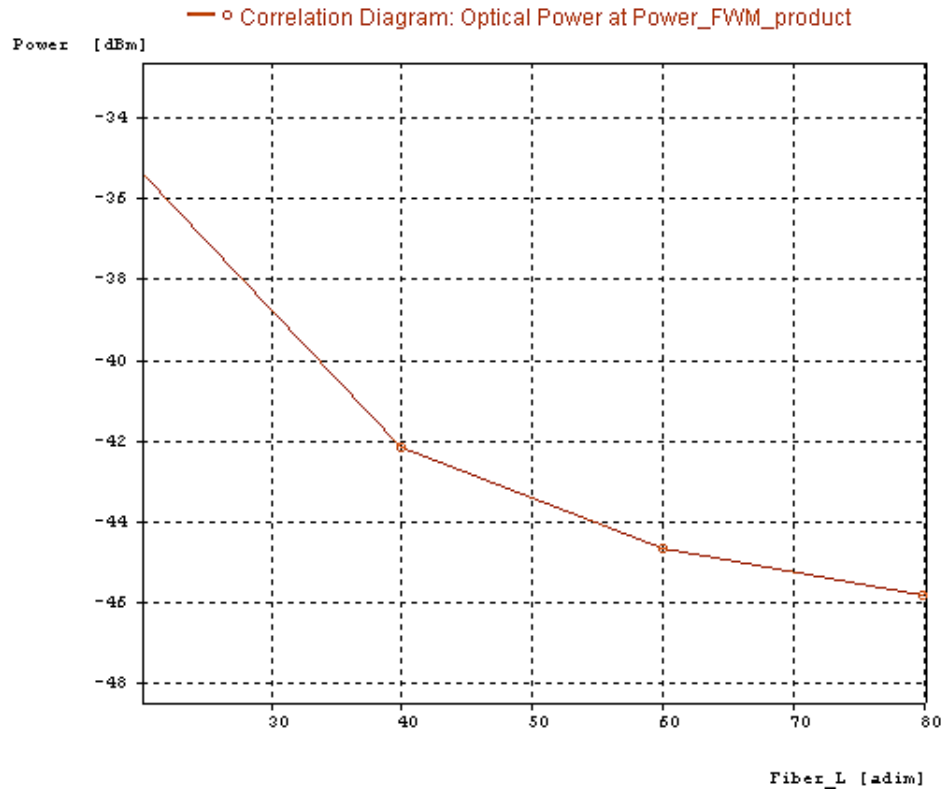


Fig. 4.24: FWM power Vs fiber length

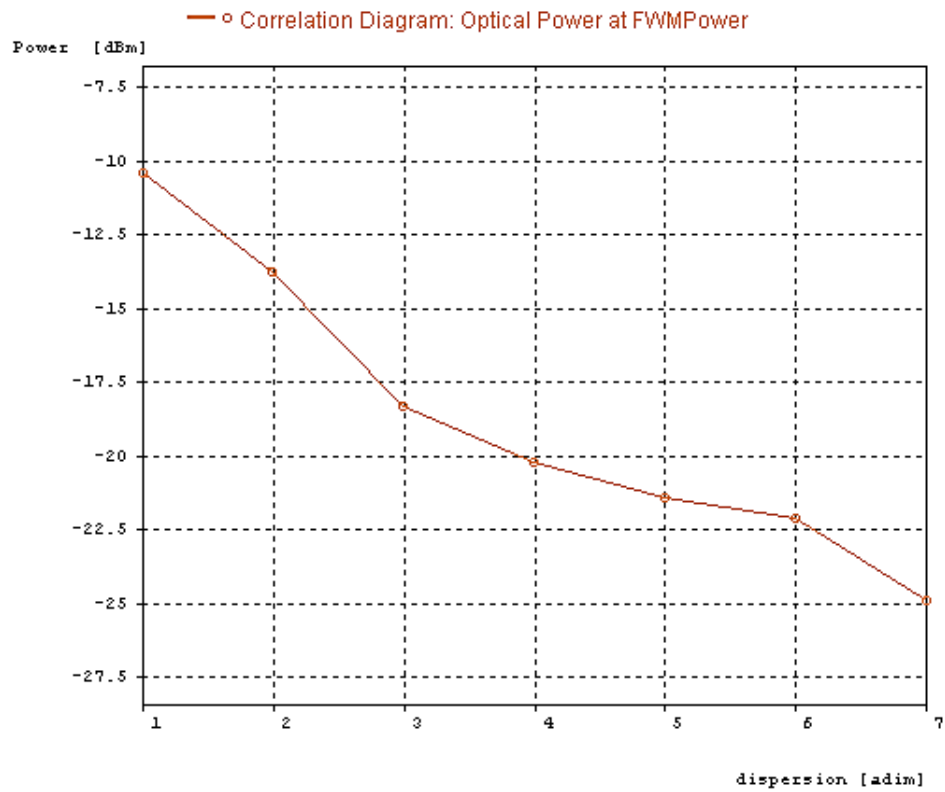


Fig. 4.25: FWM power Vs Dispersion

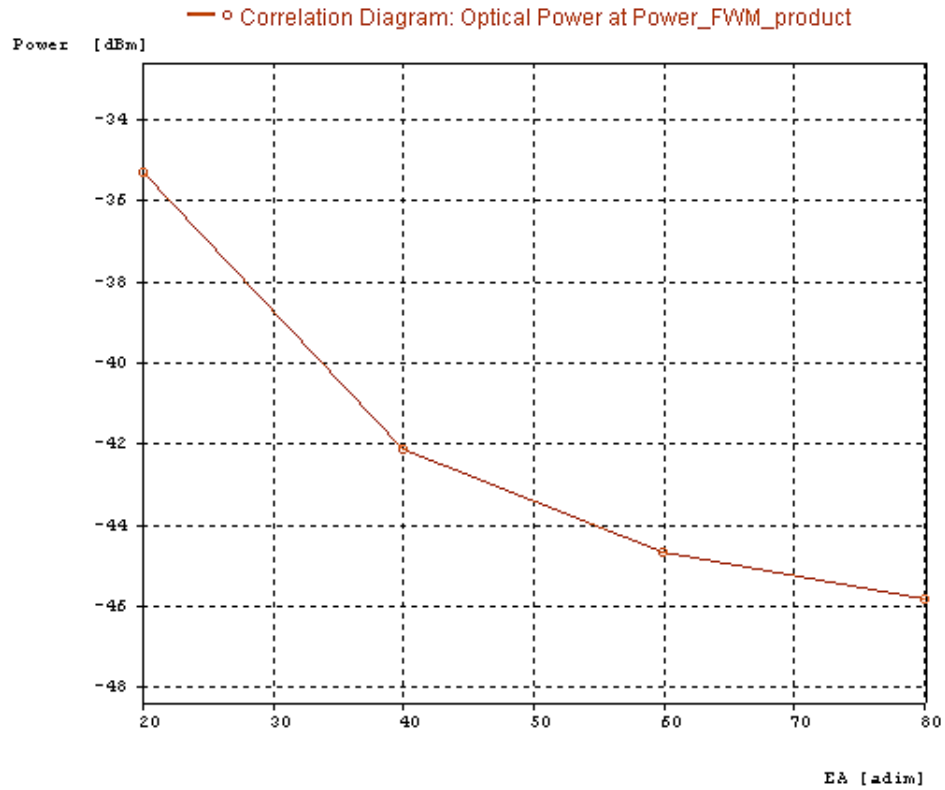


Fig. 4.26: FWM power Vs Effective area

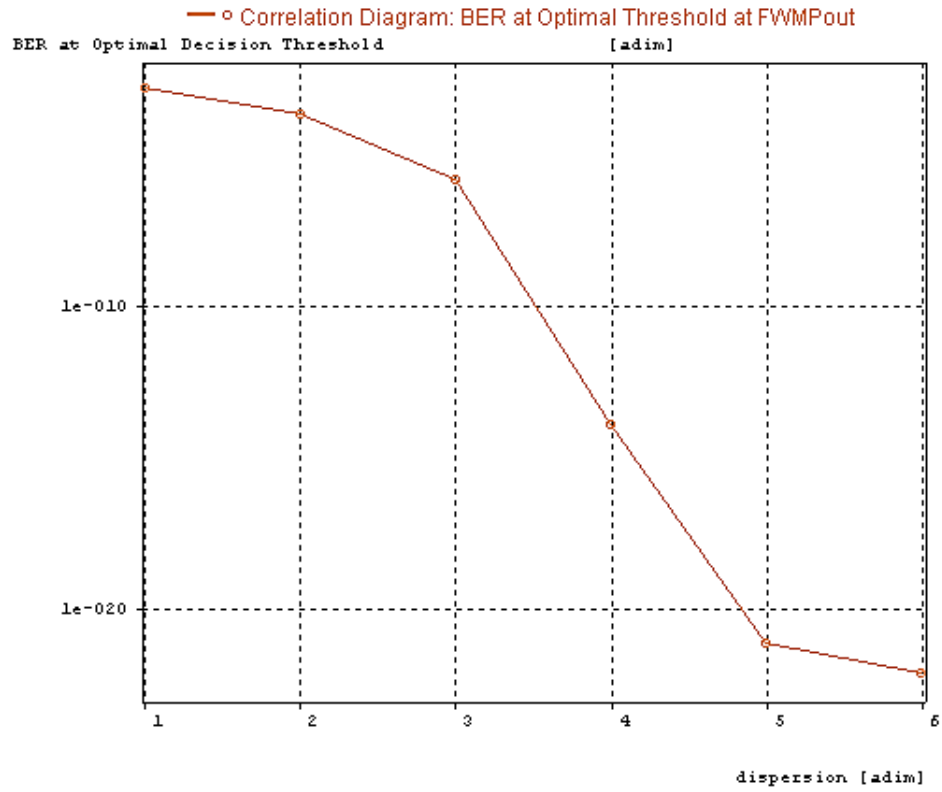


Fig. 4.27: Calculation of BER on FWM

4.9 Comparison with simulation results

In the following Fig. 4.28, Fig. 4.29 and Fig. 4.30 shows the analytical results for the comprehensive model and the results of simulation by OPTSIM are plotted in a single plot area for comparing the variation of the FWM effect. In Fig. 4.28 shows that FWM crosstalk power reduces in higher channel spacing but our comprehensive model give much better effectiveness to reduce FWM power by choosing proper system parameters. In Fig. 4.29 plots FWM power against dispersion. And in Fig. 4.30 shows the FWM power reduces when effective area of the increases. In both cases, our comprehensive model gives netter results in terms of reducing FWM crosstalk because, in comprehensive model consider all the system parameters whereas the simulation OPTSIM use a few system parameter to shows the effect of FWM.

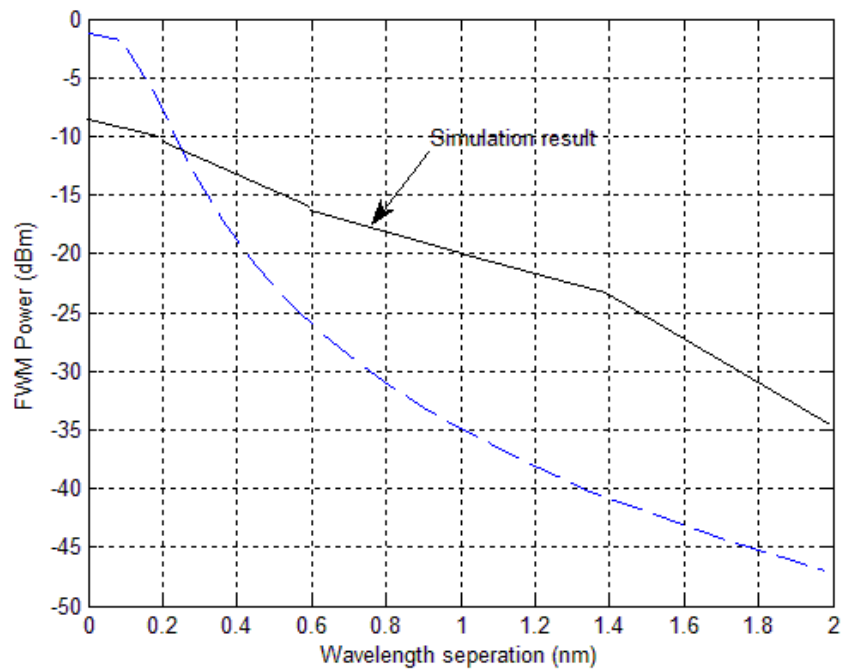


Fig. 4.28: Comparison of FWM power versus channel spacing with simulation result

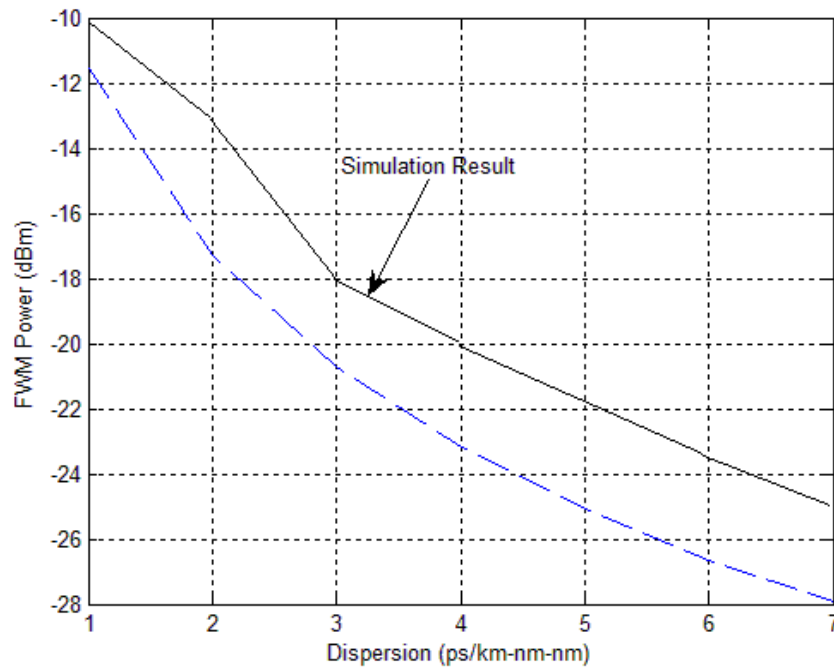


Fig. 4.29: Comparison of FWM power versus Dispersion with simulation result

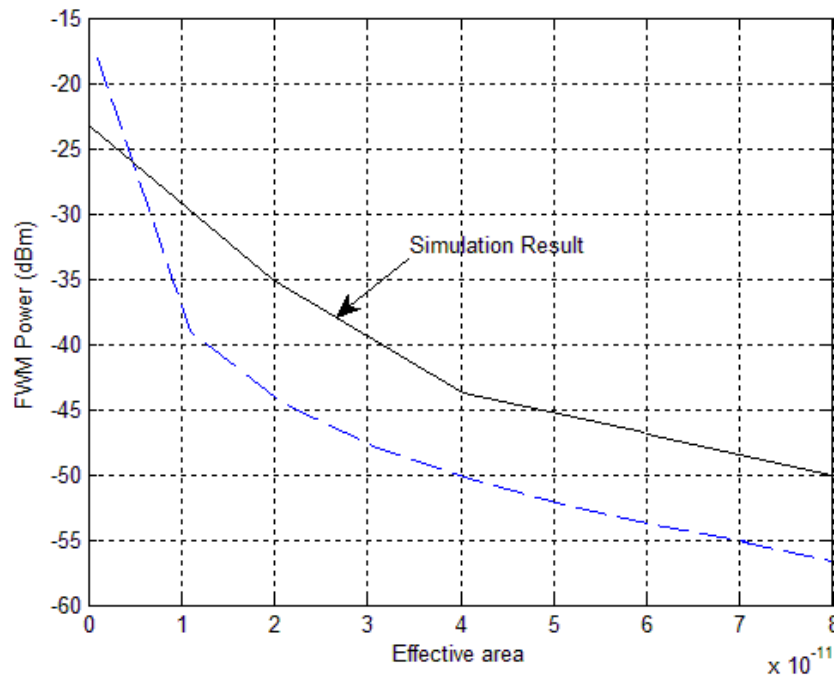


Fig. 4.30: Comparison of FWM power versus effective area with simulation result

4.10 Comparison with the published works

Many experiments and investigation has been carried out using different analysis techniques and tools to understand the FWM effect on WDM transmission system. But few works has been done to understand comprehensiveness of FWM effect. These research works mainly carried out to study the FWM effect for three different types of fiber like SSMF, DSF and LEAF with all system parameters of WDM. In this research works we also make a comprehensive model with FWM suppression parameters where we incorporate all system parameters that affect the FWM process. Other research works only noticed the effect of FWM with few design parameters. Here we have made a comparison of our research work with other published works.

Kaler et al. at [28] has shown through simulation that the FWM signal power decreases with increasing dispersion and core effective area. We simulate the plot with same parameters value in our model in Fig. 4.28 and Fig. 4.29 which coincide with the paper works and get similar trends of suppression of FWM.

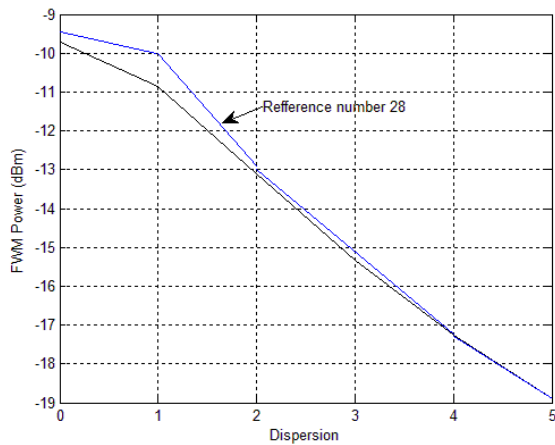


Fig. 4.31: FWM signal against dispersion for equal spaced channel on comprehensive model

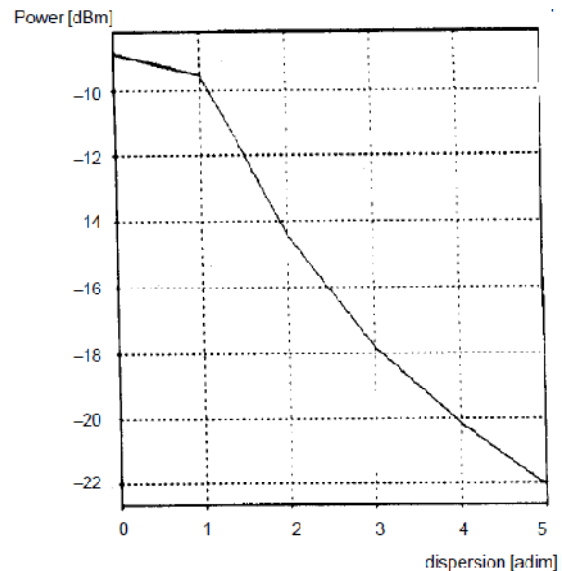


Fig. 4.32: FWM signal against dispersion for equal spaced channel in compared paper [28]

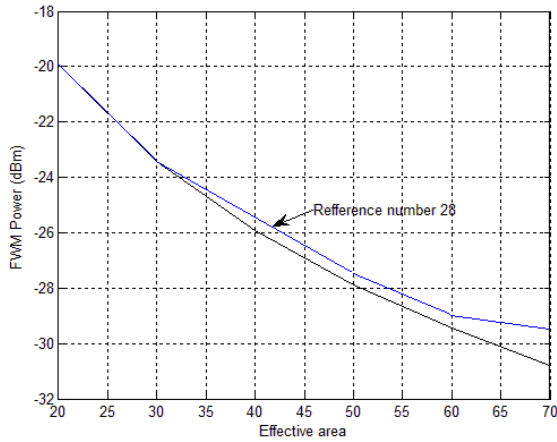


Fig. 4.33: FWM signal against core effective area for equal spaced channel on comprehensive model

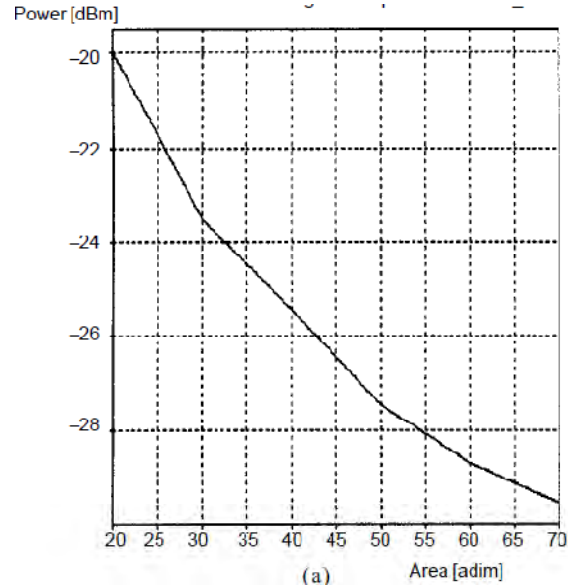


Fig. 4.34: FWM signal against core effective area for equal spaced channel in compared paper [28]

Amarpal et al at [25] has shown the FWM effect in WDM transmission for higher order of dispersion. He shows up to fifth order dispersion effect on FWM. In our model we calculate only second order dispersion parameter. Though, we get same trend of plot at Fig. 4.30 as we found in the paper [25].

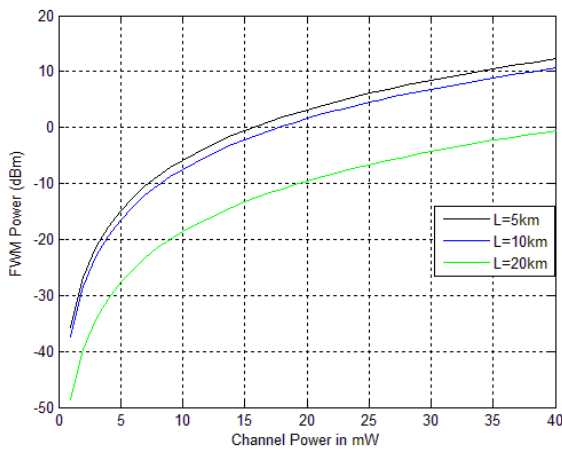


Fig. 4.35: FWM power versus input channel power at different values of core effective area under the effect of only β_3 on comprehensive model

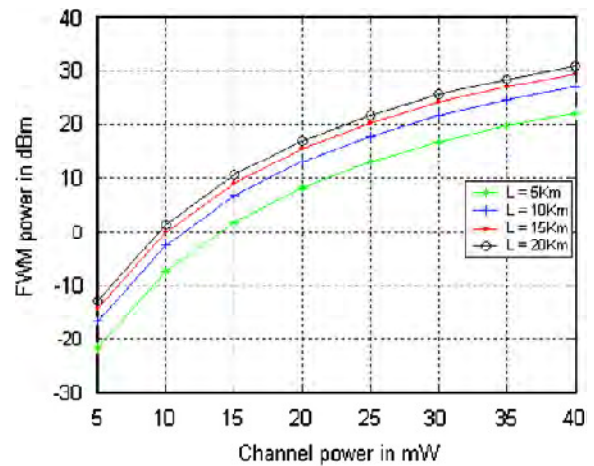


Fig. 4.36: FWM power versus input channel power at different values of core effective area under the effect of only β_3 in compared paper [25]

Li Wang et al at [26] simulated different fiber like DSF, NRZ-DSF, DCF-A with SPM, CPM and FWM effect. In our model we only consider FWM effect. We calculate FWM against input power and fiber length at Fig. 4.31 and Fig. 4.32 according the parameters values used by [26] and we observed that our plot coincide with the original plot sketched in [26].

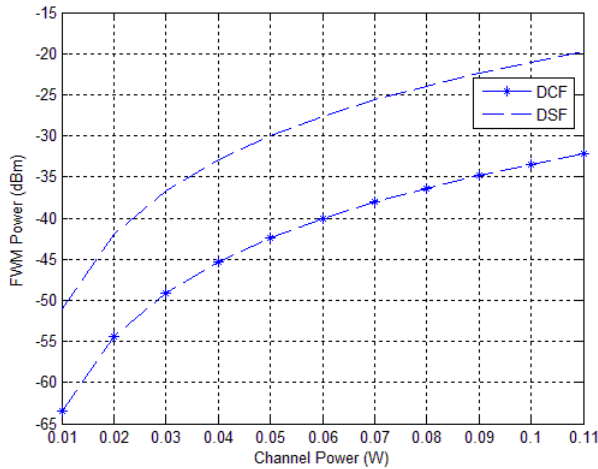


Fig. 4.37: Relation curves of FWM power and pump power on comprehensive model

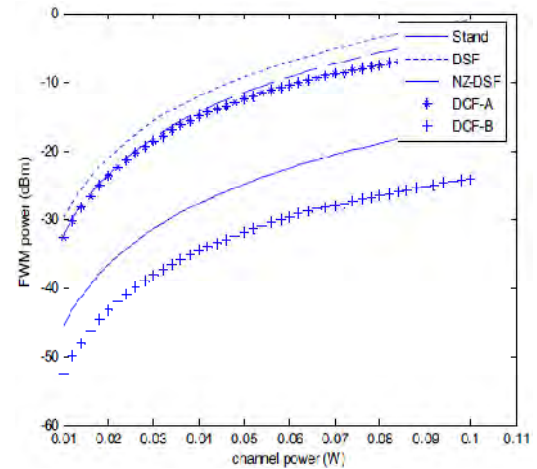


Fig. 4.38: Relation curves of FWM power and pump power in compared paper [26]

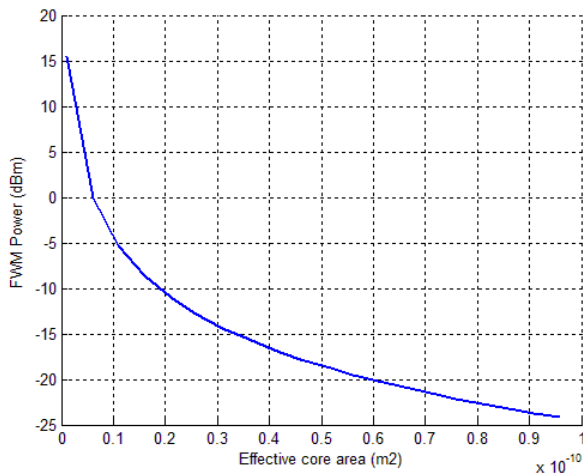


Fig. 4.39: FWM power and effective core area on comprehensive model

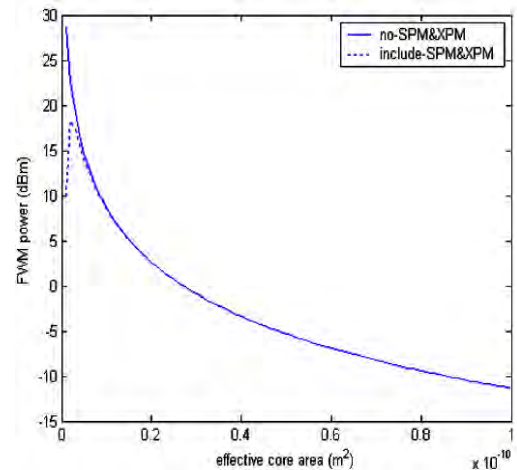


Fig. 4.40: FWM power and effective core area in compared paper [26]

Table 4.2: Comparison among different related research works.

Ref. of research works	Type of research works	Fiber used for research	System Parameters used	Performance of FWM suppression
Kamal et al. (2004) [29]	Simulation	General/modified Standard	Dispersion, Channel spacing, Core effective area	At higher dispersion, $D_c = 5$, get -22dBm of FWM and at $A_{eff} = 50\mu m^2$ FWM suppressed -27 dBm. Fig. 4.18 shows the screen shot of the reference paper.
Amarpal et al. (2007) [28]	Analytical	DSF	Dispersion	At high order chromatic dispersion with high input gets robust amount of FWM.
Shuxian et al. (2008) [25]	Analytical	modified Standard	Channel spacing, Core effective area	At $\Delta\lambda = 0.5nm$. gets FWM at -15dBm. Fig 4.19 shows result of the original paper.
Laxman et al. (2011) [24]	Simulation	DSF	Channel spacing	Shows the higher channel spacing reduces FWM effect but bit error rate is too high at 10^{-16} .
In this research work	Analytical and design a comprehensive model for FWM suppression	SSMF, DSF, LEAF	Dispersion, Channel spacing, Core Effective area, fiber length, channel input power.	At $D_c = 5$, we have the FWM power around -30dBm to -40dBm. With $\Delta\lambda = 1.6 nm$, FWM is at -57dBm for SSMF fiber. For the same channel spacing, FWM is -20dBm to -30dBm.

4.11 Discussion

A detailed computation and results analysis is carried out to evaluate the impact of FWM in WDM system for different compensating parameter of optical fiber. Results are evaluated and compared for commercially available SSMF, DSF and LEAF. We observed that FWM has more impact on DSF and LEAF fiber than that of SSMF.

It has been shown that FWM effect can be suppressed by increasing dispersion in the fiber. There is less FWM effect if wider spaced channels are considered. Further with increase in effective area of the fiber, the FWM effect can be reduced. It is also found that at higher channel spacing and effective area reduces the FWM effect on all kind of fibers and higher input power of the channel increases the FWM power. We also observed that chromatic dispersion coefficient and group velocity dispersion are inter-related. We found higher dispersion of the fiber decreases the FWM effect on fiber.

4.12 Summery

In this chapter all the fiber categories has been simulated according to the analytical results and OPTSIM simulation results. And also analyzed the results with appropriate manner and justified the model results with comparison of other published results. Hence, comparative illustration has been shown in this chapter.

CHAPTER 5

Conclusion and Future Work

5.1 Conclusion

The main motivation of this work is to obtain a comprehensive analytical model to characterize the effect four wave mixing (FWM) fiber nonlinearity on fiber optic communication systems. Fiber nonlinearities have become one of most significant limiting factors of system performance since the advent of erbium-doped fiber amplifiers because input power is increasing and the effects of fiber nonlinearities are accumulating with the use of optical amplifiers. In wavelength-division-multiplexing (WDM) systems, inter-channel interference due to fiber nonlinearities especially FWM may limit the system performance significantly. Therefore, understanding of FWM is crucial to optimize system performance of optical fiber transmission links. However, very few limited analytical models exist to analyze the effects of FWM crosstalk. Conventionally, pure numerical methods have been used to study FWM crosstalk. It is important to have an analytic model for the FWM to estimate and minimize the impact of FWM for a given transmission system design. In this thesis, an comprehensive analytical model has been presented to give better physical insight of the effect of FWM crosstalk on fiber optic communication systems. The major results obtained from each approach are summarized as follows:

1. From analysis and numerical simulation we have found that with the increase of input power the FWM crosstalk increases. Depending on the fiber type, FWM crosstalk power generation is different under some constant system parameters. Again, amount of FWM power of dispersion shifted fiber (DSF) and large effective area fiber (LEAF) is about 20% greater than standard single mode fiber (SSMF). It is further observed that with the increase of dispersion the FWM effect is decreases. Again efficient channel spacing consideration will decreases the FWM effect in SSMF fiber than that of DSF and LEAF.
2. The FWM crosstalk power is strongly depends on effective area and channel spacing, *i.e.* at lower effective area and narrow channel spacing, the crosstalk effect becomes higher. For the different fibers, the FWM effect is minimum in SSMF and maximum in DSF in WDM optical communication system.

3. FWM crosstalk power is lower in higher dispersion and higher spaced channel of pump power but it increases with the increasing the input power and fiber length.
4. It is noticed that the FWM also causes inter-channel cross talk for equally spaced WDM channels. Thus, FWM can be mitigated using unequal channel spacing.
5. The numerical simulation model results and the analytical model results were compared. The numerical simulated results clearly demonstrate that the degradation due to FWM can be minimized by proper choosing of system parameters.

Finally, it could be concluded that results obtained from this study will provide useful information for identifying the fundamental limit of the capacity of the WDM systems due FWM.

5.2 Recommendations for Future Work

Research work is a continuous process. So it is very important to think about the scope of further extension of this work. In this research work we have considered the system parameters which affect the generation of FWM for three channels. Further consideration like channel choosing technique and modulation technique can be considered. So future research work related to our work can be done as in the following direction.

1. Modulation technique can be applied to understand the behavior of FWM process in WDM system.
2. Unequal channel spacing and their selection method for transmission should be done for observing the model behavior.
3. Other nonlinear effects may be also considered to reflect the true performance limitations due to nonlinear phenomenon.
4. It is also can be analyze the BER for core effective area and dispersion to find the suppression level of FWM.
5. Higher order of dispersion may have effect on FWM suppression. So it should be done to understand the model performance and accuracy.

5.3 Summery

In summary, effect of FWM may have positive or negative on WDM system performance; depending on its application in practical field. So, further research works should be carried out to find out the roles of FWM by using different design and analysis methods.

REFERENCES

1. Tomoaki O. and Iwao S., "Optical Synchronous CDMA, Encyclopedia of Telecommunications" Editor: John Proakis, John Wiley & Sons, Inc, April, 2003.
2. Mendez A.J., Gagliardi R.M., Hernandez V.J., Bennett C.V., and Lennon W. J. , "Design and performance analysis of wavelength/time (W/T) matrix codes for optical CDMA," IEEE Journal of Lightwave Technology, vol. 21, no. 11, pp. 2524-2533, November 2003.
3. Agrawal G.P. "*Nonlinear fiber optics*" Academic Press, San Diego, C.A, 2005.
4. Senior J.M., "*Optical fiber communications*," Prentice Hall, New Delhi, 2002.
5. Keiser G., "*Coherent Optical Fiber Communications*," Optical fiber communications, McGraw-Hill, Newyork, 1991.
6. Sugahara H., Kodama, "Optimal dispersion management for wavelength division multiplexed RZ optical pulse transmission," Electronic Letters, vol 34 no. 9, pp. 902-904, April 1998.
7. Forghieri, F, Tkach, R.W and Chraplyvy, A.R., "Fiber nonlinearities and their impact on transmission systems", in Optical Fiber Telecommunications IIIA, I.P. Kaminov and T.L. Koch, Eds. San diego, CA, Academic Press, March, 2005.
8. Hussam G. Batshon, Ivan B. Djordjevic and Bane V. Vasic, "An improved technique for suppression of intrachannel four-wave mixing in 40-Gb/s optical transmission systems.", IEEE Photonics Technology Letters, vol. 19, no. 2, pp. 67 – 69, January, 2007.
9. Forghieri, F, Tkach, R.W and Chraplyvy, A.R., "Reduction of four-wave mixing crosstalk in WDM systems using unequally spaced channels", IEEE Photonics Technology Letters, vol. 06, no. 6, June, pp. 118-120, 1994.
10. John Z. and Curtis R. Menyuk, "Reduction of intra-channel four-wave mixing using subchannel multiplexing", IEEE Photonics Technology Letters, vol. 15, no. 2, pp. 323 – 325, February, 2003.
11. Mussot A., Lantz E., Durecu-Legrand A., Simonneau , Bayart D., Maillotte H. and Sylvestre T., "Simple method for crosstalk reduction in fiber optical parametric amplifiers", Proceedings of European Conference on Optical Communications (ECOC), pp. 1-2, September, 2006.
12. Kao, K.C. and Hockham, G.A., "Dielectric fiber surface waveguides for optical frequencies." Proceedings of IEE Journal of Optoelectronics, vol. 133, no. 3 pp. 191 - 198, June, 1986.
13. Colas, T. M., Green, M., Wuzniak, G. and Arena, J., "The TAT-12/13 cablenetwork" IEEE Communication Magazine, vol. 34, no.2, pp. 24-28, 1996.

14. Barnett W.C., Takahira H., Baroni G. C. and Ogi., “ The TPC-5 cable network.”, IEEE Communication Magazine, vol.34, no.2, pp. 24-28, 1996.
15. Sharif, M. and Alkhansari M. G., “On the peak to average power OFDM signals based on over sampling”, IEEE Transactions on Communications, vol. 51, no. 1, pp. 72-78, 2004.
16. Bernhard G. and Norbert H., “Analytical Calculation of the Number of Four-Wave-Mixing Products in Optical Multichannel Communication Systems” Technical report, Technical University of München, Germany, October, 2008.
17. Kaler R. S., Sharma A.K. and Kamal T. S., “Approximate and exact small signal *analysis* for single-mode *fiber* near zero-dispersion wavelength including higher-order dispersion terms”, Journal of Fiber and Integrated Optics , vol 21, no. 5 pp. 391-415, November, 2010.
18. Gurmeet K., Singh M.L. and Patterh M.S., “Simulation of GBPS DWDM transmission system in the presence of fiber nonlinearities”, Proceedings of International Conference on Optics and Photonics, pp. 1-4, November, 2009.
19. Rajneesh R., Sahal A., Kale R.S. r, “Optimum algorithm for WDM channel allocation reducing four-wave mixing effects”, International Journal for Light and Electron Optics, vol. 120, no. 17, pp. 898-904, November, 2009.
20. Hussam G. Batshon, Ivan B. Djordjevic and Bane V. Vasic, “An improved technique for suppression of intrachannel four-wave mixing in 40-Gb/s optical transmission systems.”, IEEE Photonics Technology Letters, vol. 19, no. 2, pp. 67 – 69, January, 2007.
21. Ramprasad A. V. and Meenakshi, M. “A theoretical Approach to analyze impact of FWM on DWDM systems”, Academic Open Internet Journal, vol. 17, no. 1, pp. 2, 2006.
22. Nordiana M S., “Nonlinear Optical Effects Suppression Methods in WDM System with EDFAs: A Review”, Proceedings of International Conference on Computer and Communication Engineering (ICCCE), pp. 1-4, May, 2010.
23. Ming-Jun L., Xin C., Anping L., Stuart G., Ji W., Donnell T. W., Luis A. Z.,” Effective area limit for large mode area laser fibers” Proceedings of Optical Fiber Communication Conference (OFC), vol. 26, no. 14, pp. 1-3, February, 2008.
24. Laxman T., Shantanu J., Premanand K., and Shankar D., “Investigation Of Fwm Effect On BER In WDM Optical Communication System With Binary And Duobinary Modulation Format”, International Journal of Distributed and Parallel Systems (IJDPS) Vol.1, No.2, pp. 15-19, November 2010.

25. Singh A., Sharma A.K. and Kamal T. S., "Four-wave mixing analysis in WDM optical communication systems with higher-order dispersion", *International Journal for Light and Electron Optics*, vol. 119, no. 16, pp. 788–792, December, 2008.
26. Li W., Wenzheng B., Yang S., Jiangbo C., and Xinping Z., "Effect of FWM output power induced by phase modulation in optical fiber communication", *Proceedings of PIERS*, vol. 21, pp. 1874 August, 2009.
27. Stallings, W. "Data and Computer Communications", Pearson Education, Inc., pp.247-248, 2007.
28. Kaler R.S., "Simulation results for four wave mixing in an optical fibre near zero-dispersion wavelength", *Journal of The Institution of Engineers (India)*, pt ET, vol 85, July 2009.

OUTCOMES OF THIS RESEARCH WORK

1. **S. A. Mamun** and M. S. Islam, “Effect of Chromatic Dispersion on Four-Wave Mixing in Optical WDM Transmission System”, Proceedings of 6th International Conference on Industrial and Information Systems (ICIIS 2011), pp-430-434, held on 16th – 19th August 2011, Kandy, Sri Lanka. (http://ieeexplore.ieee.org/xpl/freeabs_all.jsp?arnumber=6038106).
2. **S. A. Mamun** and M. S. Islam, “Non-linear effect on WDM transmission system”, 2nd International Conference on Photonics (ICP 2011), held on 17th – 19th October 2011, Kota Kinabalu, MALAYSIA. (Accepted).
3. **S. A. Mamun** and M. S. Islam, “Effect of Channel spacing on Four-Wave Mixing in Optical WDM Transmission System”, 3rd International Conference on Computational Intelligence, Modelling & Simulation (CIMcim2011), held on 20th – 22th September 2011, langkawi, MALAYSIA.(Accepted).